Chapter 2
Scanning probes microscopes instrumentation

Objective: learn the general techniques that are essential for SPM.

Chapter 2
Scanning probes microscopes instrumentation

2.1: Tips

Tips geometry requirements

Strong relief: need for a small angle,
otherwise the surface is not faithfully imaged.

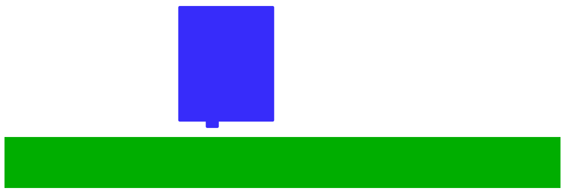

Need for atomically-sharp apex for atomic resolution on a “flat” surface, rest of the tip can be blunt.

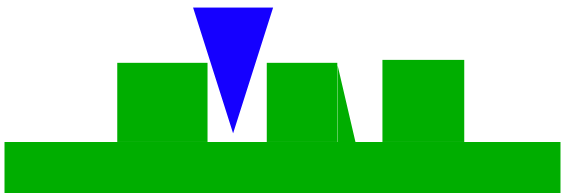

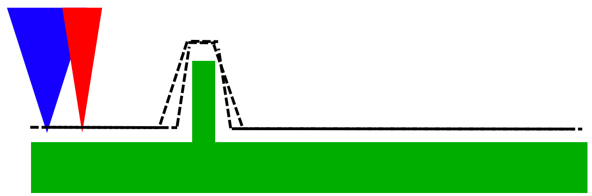

The latter point is also true for AFM and related techniques.

An artefact: tip imaging

Sample with needle-like structures: a Al_2O_3 surface imaged by AFM.

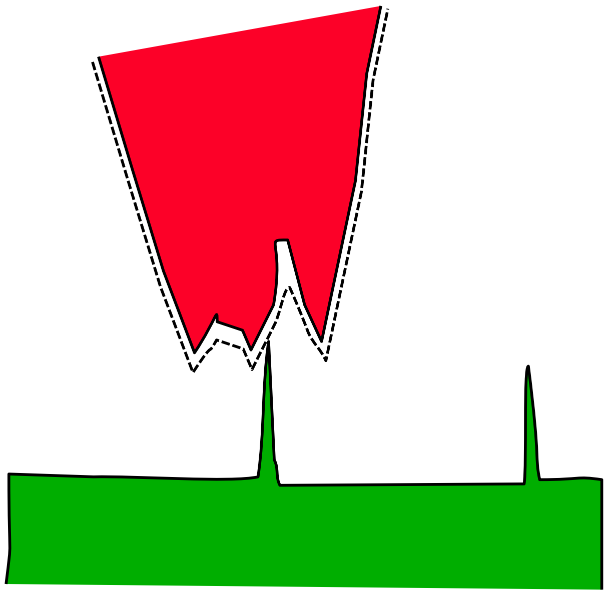

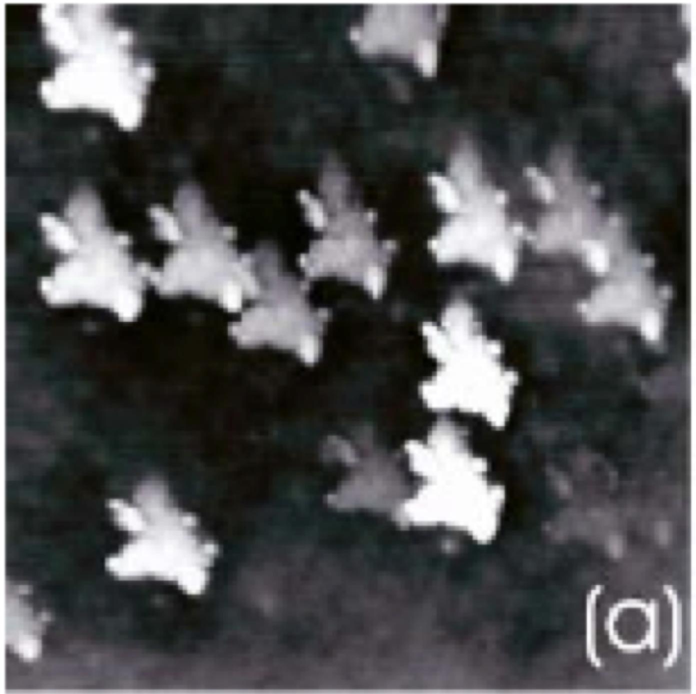

459 x 459 nm²

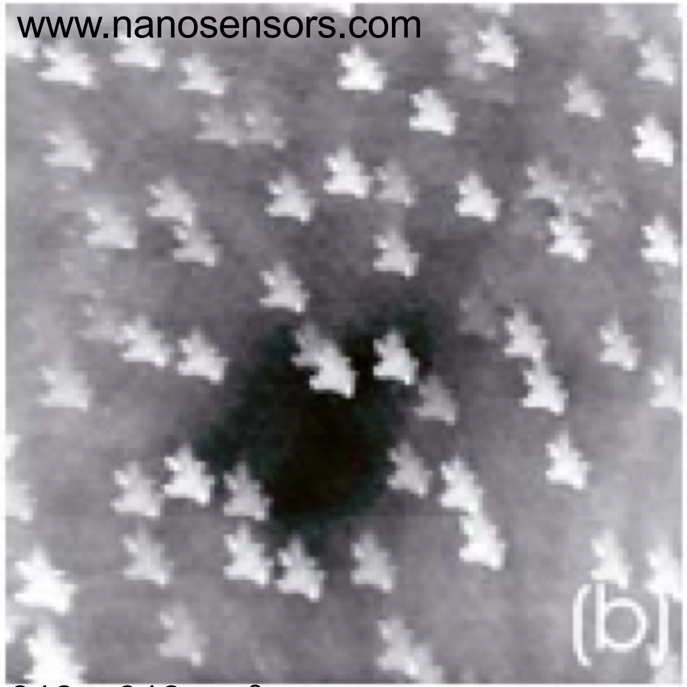

918 x 918 nm²

The blunt tip is imaged by the sharp sample needle-like structures.

Effect recognized by observation of numerous identical structures.

Different brightness due to different heights of the needles.

STM tips: materials

Criteria:
Surface quality, low oxydability,
Ease of preparation,
Rigidity.

Materials:
W: easy to etch, rigid.
Pt: very low oxydability, but soft.
Au: very low oxydability but very soft.
$Pt_{90}Ir_{10}$: good rigidity/oxydability compromise.

Tip can be simply cut from a wire. →
Electrochemistry-based recipies are more reliable.

STM tips: etching techniques

Material-dependent, W is easy.
The reactants flow governs the locality of the etch.

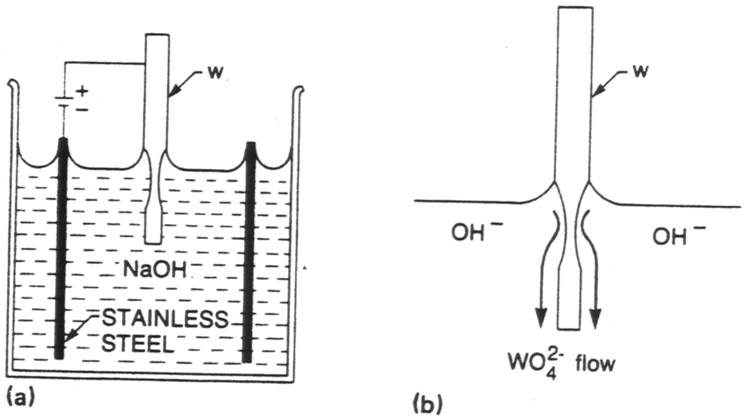

Fig. 13.1. Electrochemical etching of tungsten tips. (a) A tungsten wire, typically 0.5 mm in diameter, is vertically inserted in a solution of 1N NaOH. A counterelectrode, usually a piece of platinum or stainless steel, is kept at a negative potential relative to the tungsten wire. (b) A schematic illustration of the etching mechanism, showing the "flow" of the tungstate anion down the sides of the wire in solution. (Reproduced from Ibe et al., 1990, with permission.)

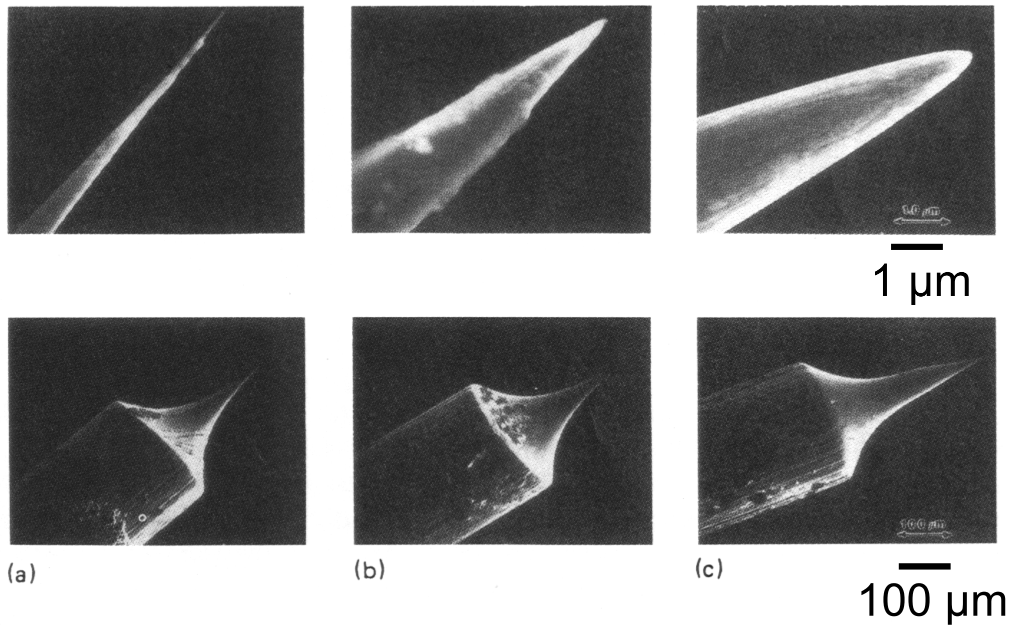

Fig. 13.2. Dependence of tip radius of curvature with cutoff time. Scanning electron micrographs of tips with different etching-current cutoff time. (a) 600 ns, with an average radius of curvature 32 nm. (b) 140 ms, with an average radius of curvature 58 nm. (c) 640 ms, with an average radius of curvature 100nm. (reproduced from Ibe et al., 1990, with permission.)

The excess etching time after the drop of the lower part has a strong influence on the final tip geometry:
Long over-etch = blunt tip.

STM tips: final preparation

Used in some specific cases.

Objectives:

Improve tip geometry, remove oxide:
- by thermal treatment: at 1000° C : 2 WO_3+ W -> 3 WO_2 volatile
- by field evaporation (atom migration)

Attach some atoms of another element (Si, Cu):
- by controlled collision

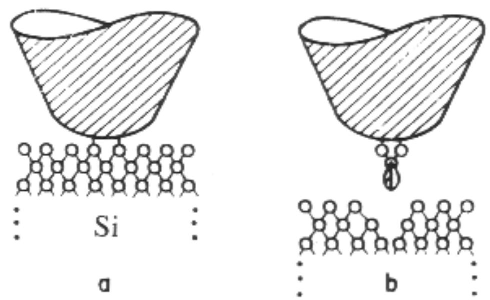

Fig. 13.11. Mechanism of tip sharpening by controlled collision. (a) The W tip picks up a Si cluster from the Si surface. (b) A Si cap forms at the apex of the tip, providing a p_z dangling bond. (Reproduced from Chen, 1991, with permission.)

Chapter 2
Scanning probes microscopes instrumentation

2.2: Basics of piezo-electricity

The piezo-electric effect

Discovered by Pierre and Jacques Curie (1880).

Expansion/contraction ⟺ electrical potential difference

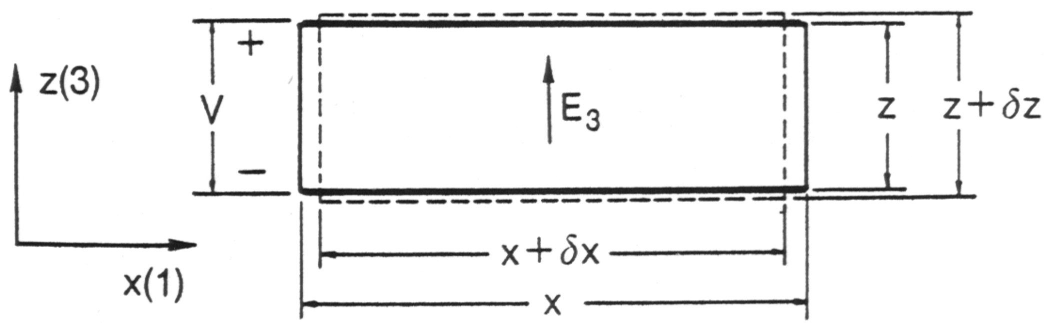

Fig. 9.3. Definition of piezoelectric coefficients. A rectangular piece of piezoelectric material, with a voltage *V* applied across its thickness, causes a strain in the *x* as well as the *z* directions. A piezoelectric coefficient is defined as the ratio of a component of the strain with respect to a component of the electrical field intensity.

Needs to be an electrically insulating material.

If z and - z are equivalent axes, no piezo-electric response.

Applications of piezo-electricity

Only some anisotropic crystals are piezo-electric: quartz, Rochette salt $KNaC_4H_4O_6$-$4H_2O$, PZT ceramics, GaAs …

Cigarette lighter, sparkers used to ignite gas stoves

Loudspeakers

Crystal resonators for frequency reference in electronics and “quartz watches”

The piezo-electric coefficients

Standard notations:

$$x \leftrightarrow 1$$
$$y \leftrightarrow 2$$
$$z \text{ (poling axis)} \leftrightarrow 3$$

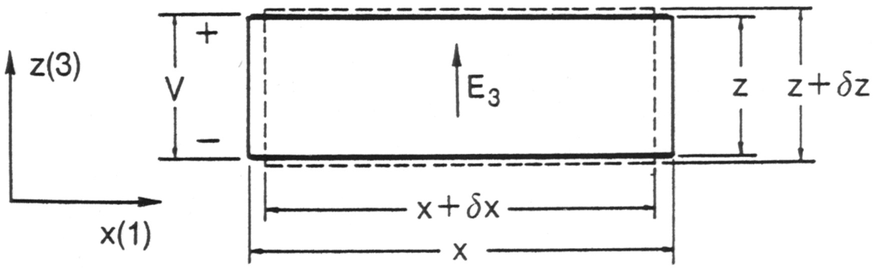

In the linear response regime:

$$\begin{pmatrix} \frac{\partial x}{x} \\ \frac{\partial y}{y} \\ \frac{\partial z}{z} \end{pmatrix} = \begin{pmatrix} d_{11} & d_{21} & d_{31} \\ d_{12} & d_{22} & d_{32} \\ d_{13} & d_{23} & d_{33} \end{pmatrix} \begin{pmatrix} E_x \\ E_y \\ E_z \end{pmatrix}$$

If voltage applied along the poling axis = 3 = z, only $d_{3...}$ are used:

$$\frac{\partial x}{x} = d_{31} E_z$$ most used mode, $d_{31} = 10^{-3}$ to 10 Å/V

$$\frac{\partial z}{z} = d_{33} E_z$$ By symmetry, usually $d_{32} = d_{31}$

The PZT materials (1)

Ceramic, solid solutions of $PbZrO_3$ and $PbTiO_3$.
Pb-Zr-Ti = PZT.

Ferro-electric with T_{Curie} about 250° C, to be used well below.

Polarization process (60 kV/cm, 1h) necessary, aligns dipoles along poling axis (z).

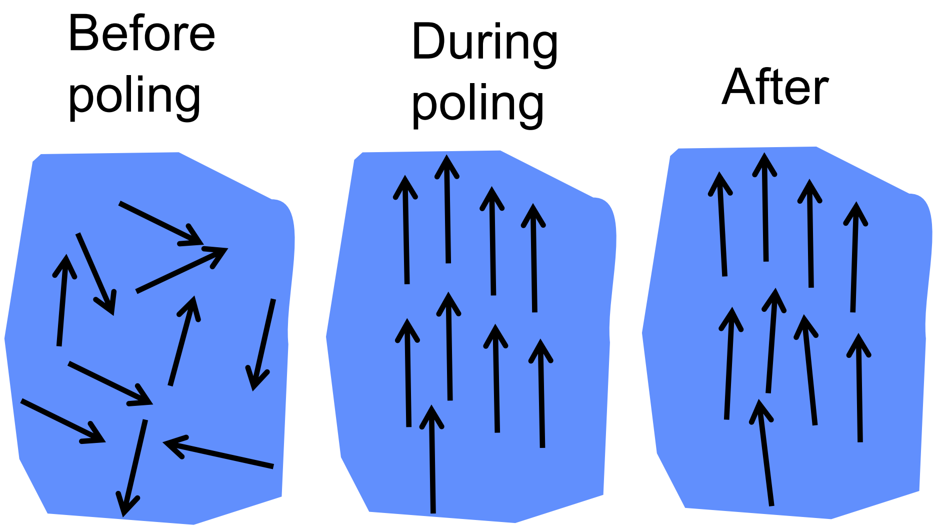

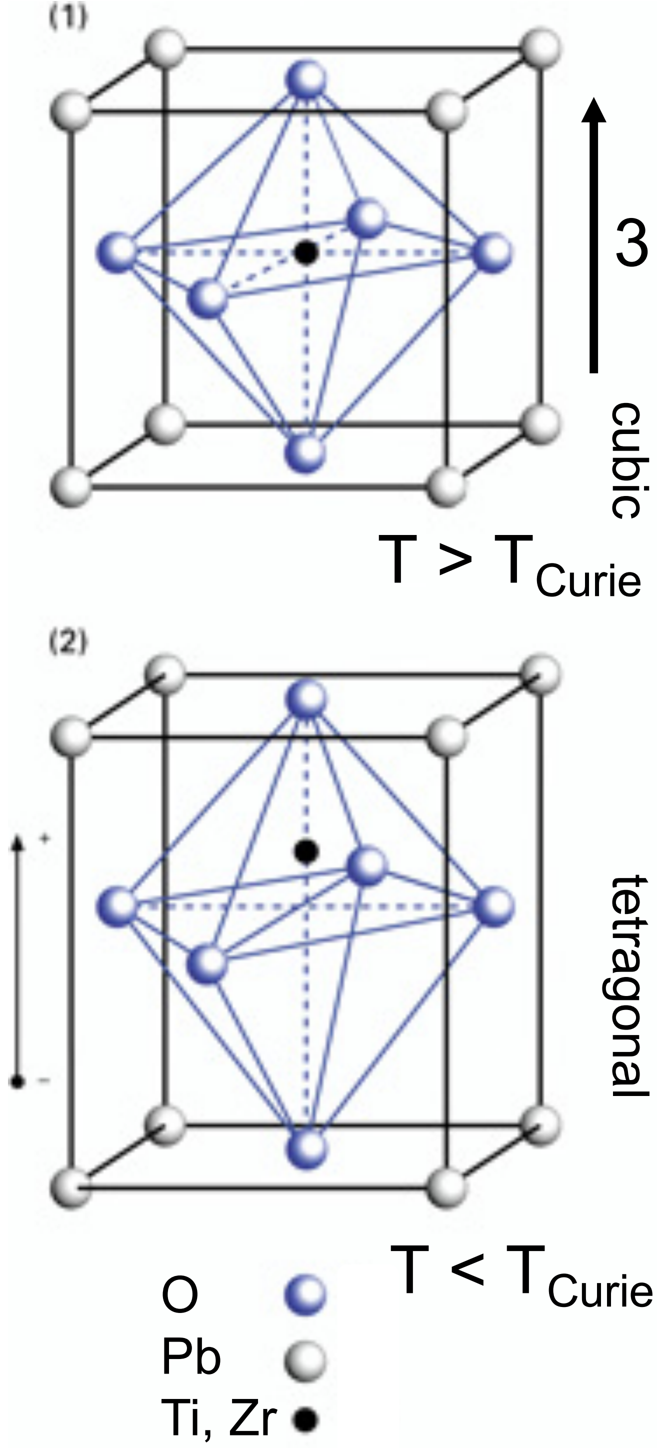

The PZT materials (2)

Piezo-electric coefficients depend strongly on composition, temperature.

d_{31} = 1-3 Å/V, d_{33} = 2-6 Å/V

dimensionless number related to the effectiveness of electrical to mechanical energy conversion.

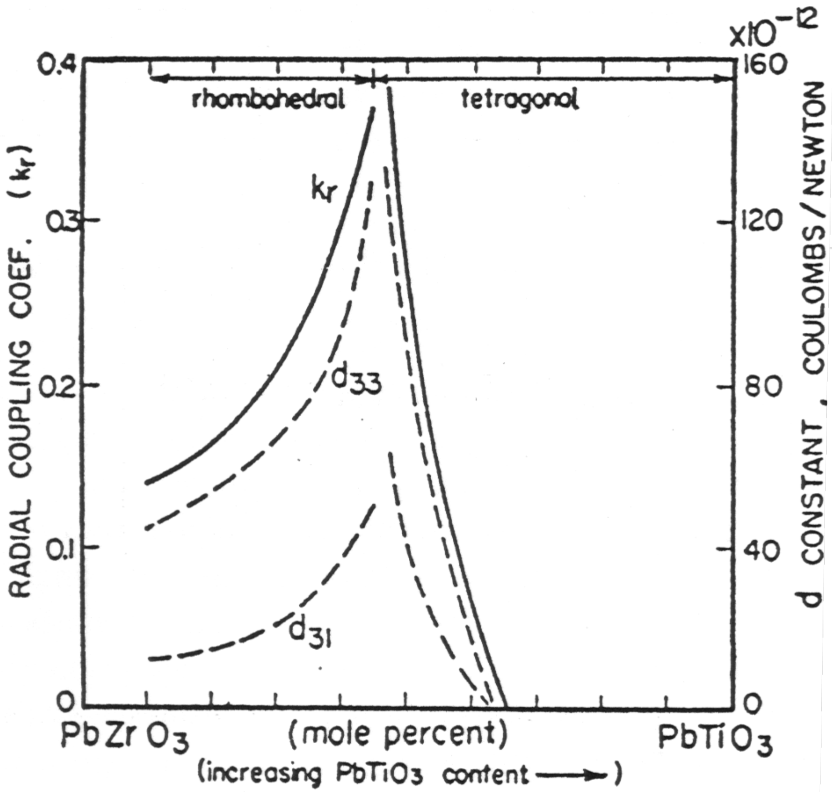

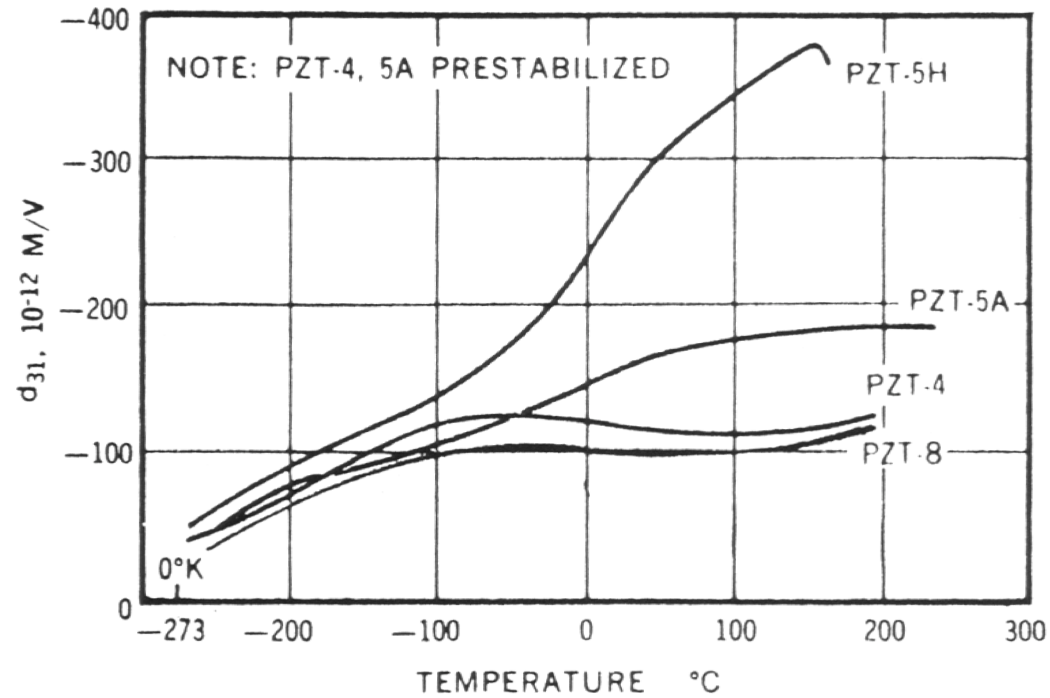

Fig. 9.5. Variation of piezoelectric coefficient with temperature. (By Morgan Matroc, Inc., Vernitron Division, Bedford, Ohio.)

Fig. 9.4. Dependence of piezoelectric properties of $PbZrO_3$–$PbTiO_3$ on composition. The zirconate-rich phase is rhombohedral, whereas the titanate-rich phase is tetrahedral. The piezoelectric coefficients reach a maximum near the morphotropic phase boundary, approximately 45% $PbZrO_3$ and 55% $PbTiO_3$. (After Jaffe et al.,

Chapter 2
Scanning probes microscopes instrumentation

2.3: Piezo-electric actuators

The tripod

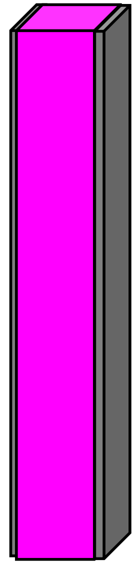

Used by Binnig et al.

Difficult to mount, not very rigid.

But easy to operate and to calibrate at the metrological level (with capacitive sensors).

A bar for every direction: $\partial L = L d_{31} E_z = d_{31} \frac{L}{e} V$

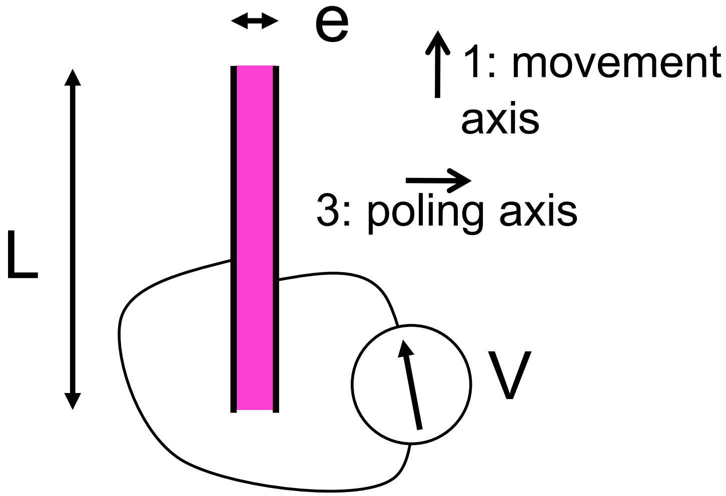

Fig. 9.6. Tripod scanner. Three PZT bars to control the *x*, *y*, and *z* displacements, respectively. The tip is mounted at the vertex of the tripod. (Reproduced from Binnig and Rohrer, 1987, with permission.)

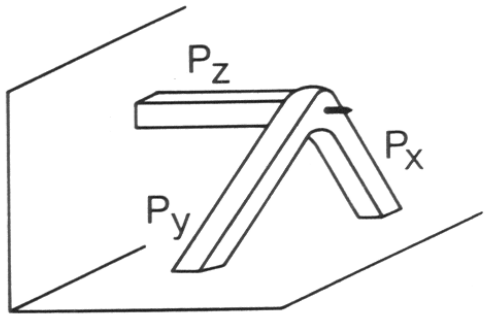

Length L = 2 cm, thickness e = 2.5 mm, V = 250 V ($E_{el} = 10^5$ V/m),
d_{31} = 2.5 Å/V
δL_{max} = 5000 Å, sensitivity = 20 Å/V

The piezo-electric tube

Inner and outer faces are metallized to form two electrodes.

Radial poling, radial electric field : axis 3 = radial direction.

Used to generate a movement in the tube axis direction..

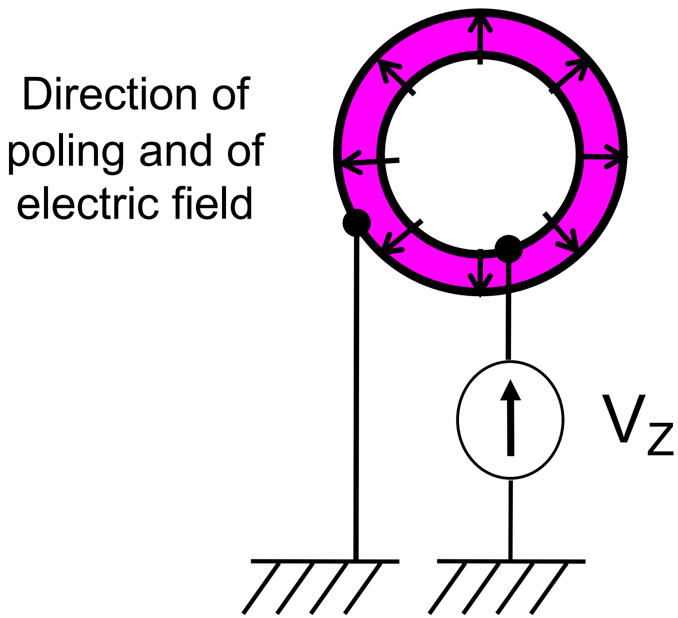

Similar sensitivity but natural rigidity of the tubular geometry.

The piezo-electric tube

$$\partial L = L d_{31} E_z = d_{31} \frac{L}{e} V$$

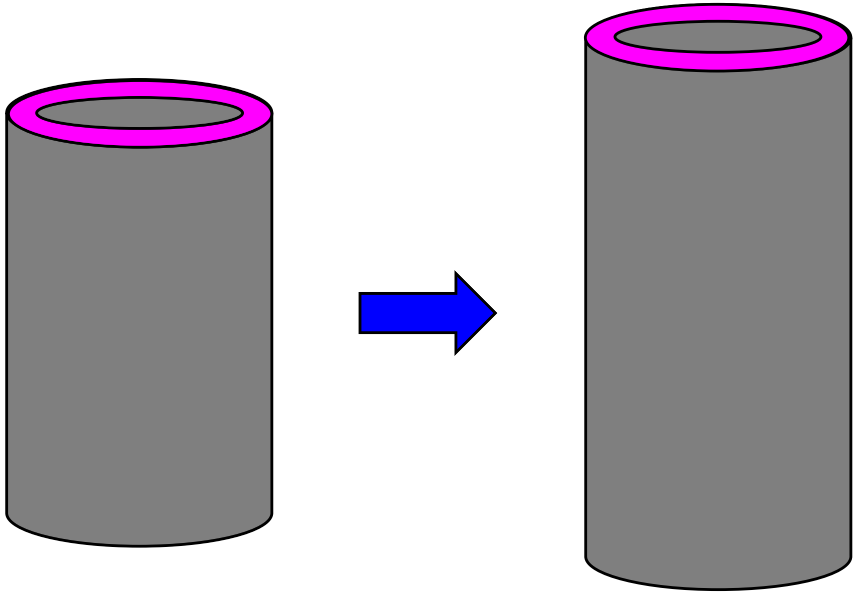

Example:

Length L = 2 cm, wall thickness e = 0.5 mm, V_{max} = 250 V (E_{el} = 5.10^5 V/m), d_{31} = 2.5 Å/V.

δL_{max} = 25000 Å = 2.5 µm, sensitivity = 100 Å/V

On drawing, deformation is much exaggerated.

The scanner tube

Tube with again radial poling.
Four quadrant electrodes on the outer face:
+ $V_{x,y}$ and – $V_{x,y}$ applied on two opposite electrodes.
Again, a voltage V_z can be applied on the (single) internal electrode.

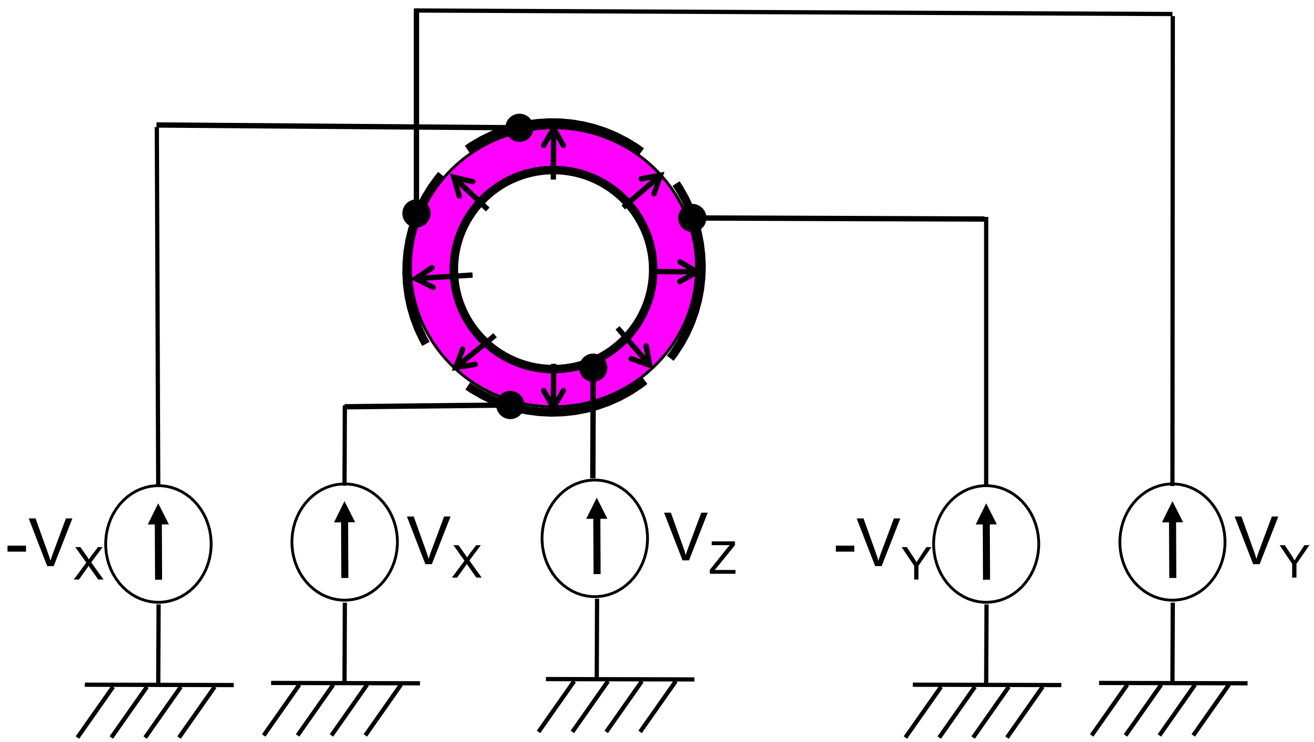

The scanner tube

$$\partial X = \frac{2\sqrt{2}}{\pi} d_{31} \frac{L^2}{De} V_X$$

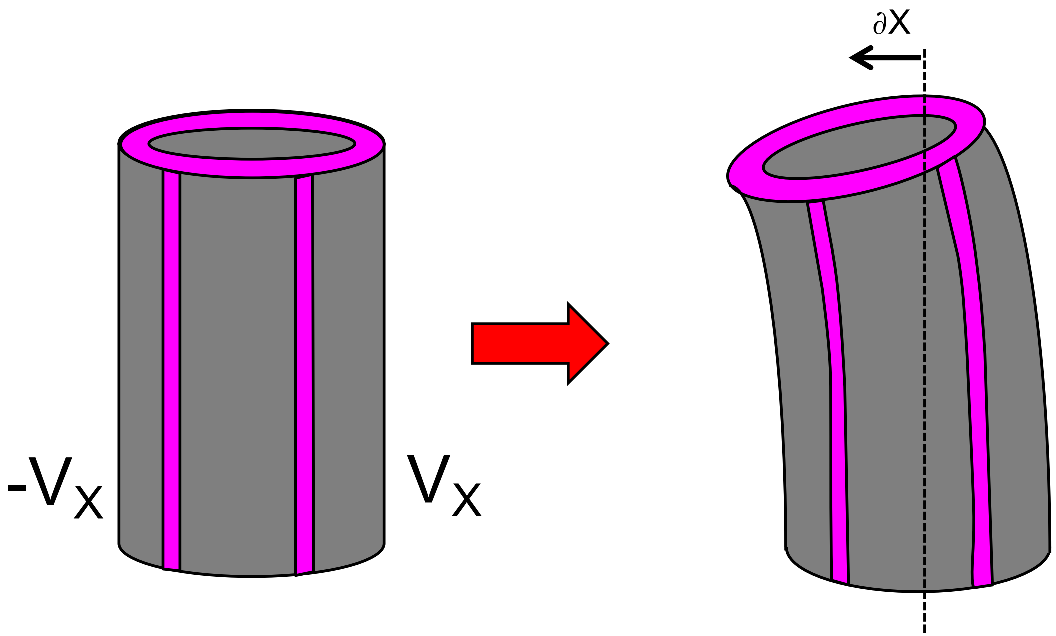

Same parameters + Diameter D = 1 cm.
δX_{max} = 50000 Å = 5 µm, sensitivity = 200 Å/V

Bow: displacement not purely lateral.
Voltage V_z applied to inner electrode: Z movement capability added.
Three movements can be done simultaneously.
Compact and quite sensitive : broadly used.

The benders

Similar effect as the scanner tube but in a single plate geometry.

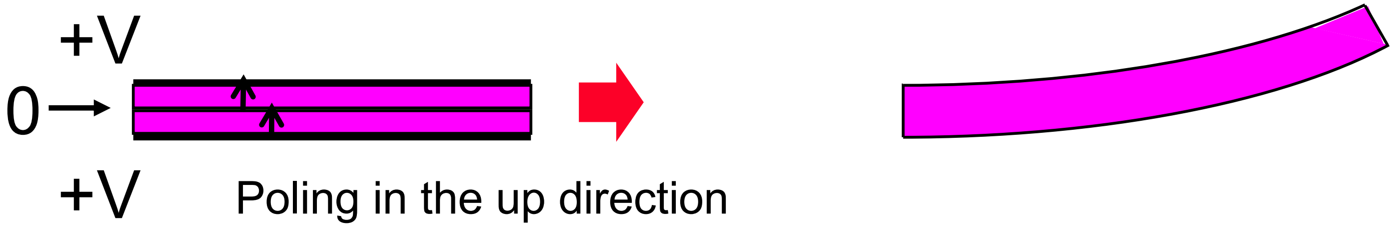

Low stiffness, force and resonant frequency.

A scanner built with 4 benders polarized in two halves: no angle with interest for laser beam reflection in AFM.

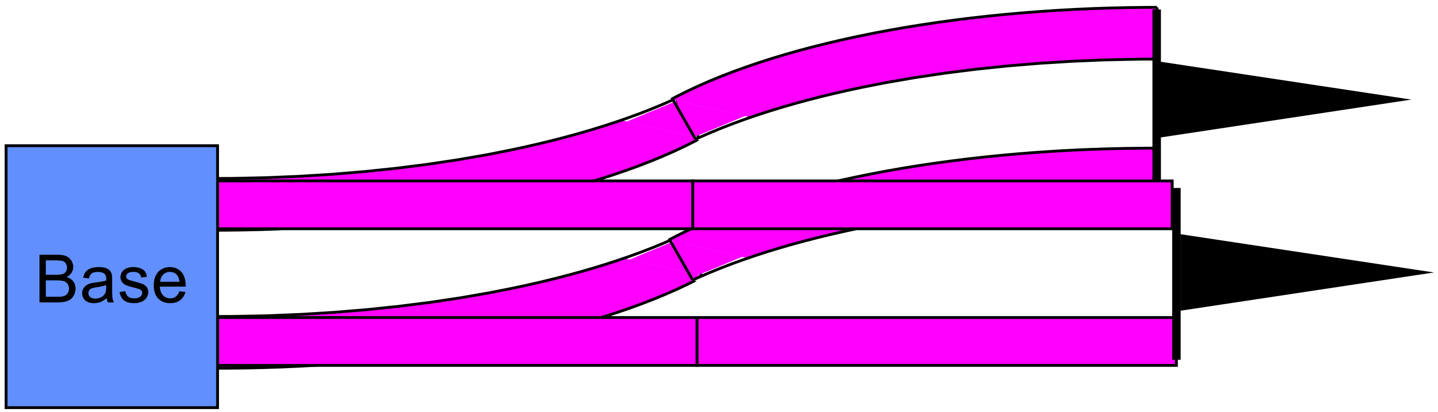

The shear piezos

The labels 4, 5 and 6 in piezo-electric coefficients describe rotations.

Here, E is applied along direction 1, perpendicular to poling.
The corresponding strain coefficient d_{15} is as high as 11 Å/V.

$$\partial X = d_{15} V$$

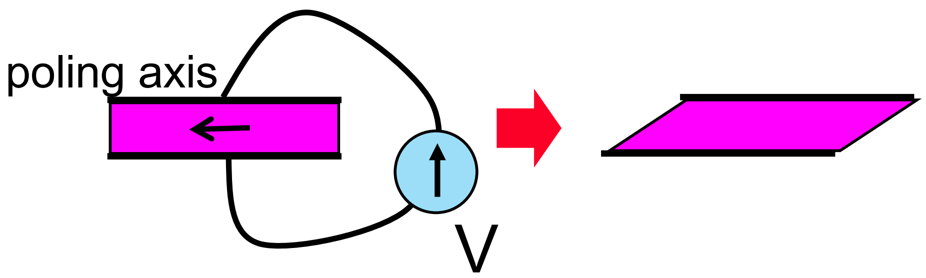

$L = 1$ mm, $V_{max} = 250$ V ($E_{el} = 2.5\ 10^5$ V/m), $d_{15} = 10$ Å/V
$\delta X_{max} = 250$ Å.

High forces, used in coarse positioning.

Fragility (it' s a ceramic !)

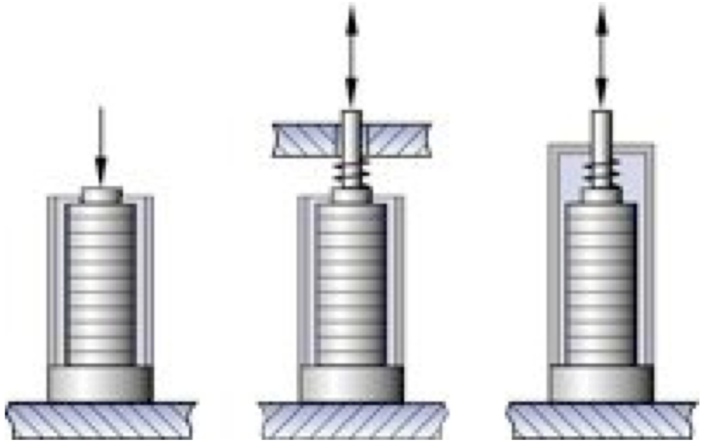

No pulling force without preload.

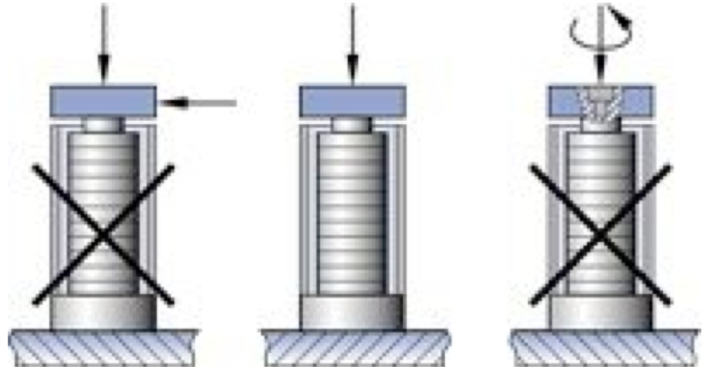

No lateral force or torque.

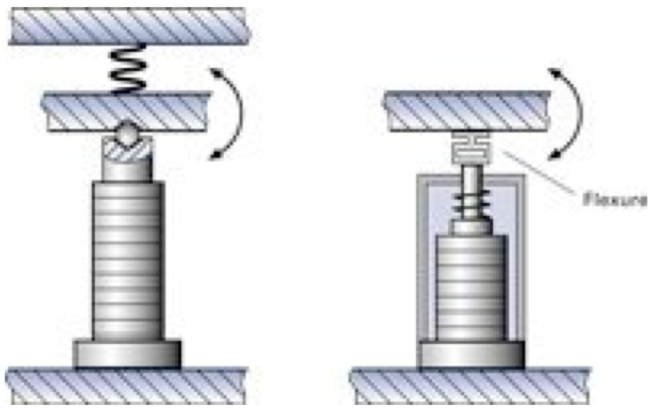

Ball tips or flexures to decouple lateral forces

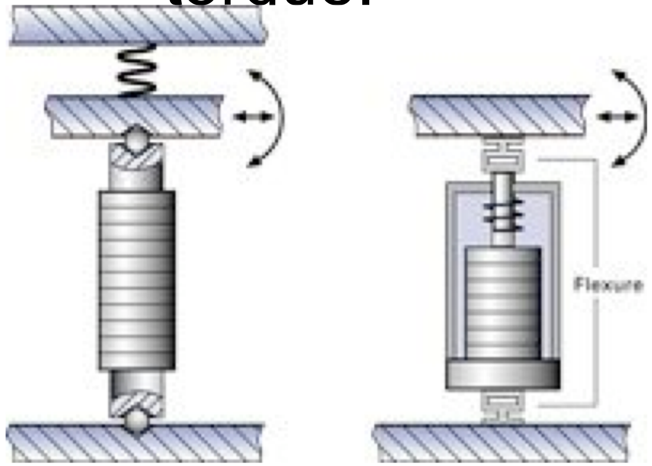

Ball tips or flexures to decouple bending forces.

Hysteresis and creep

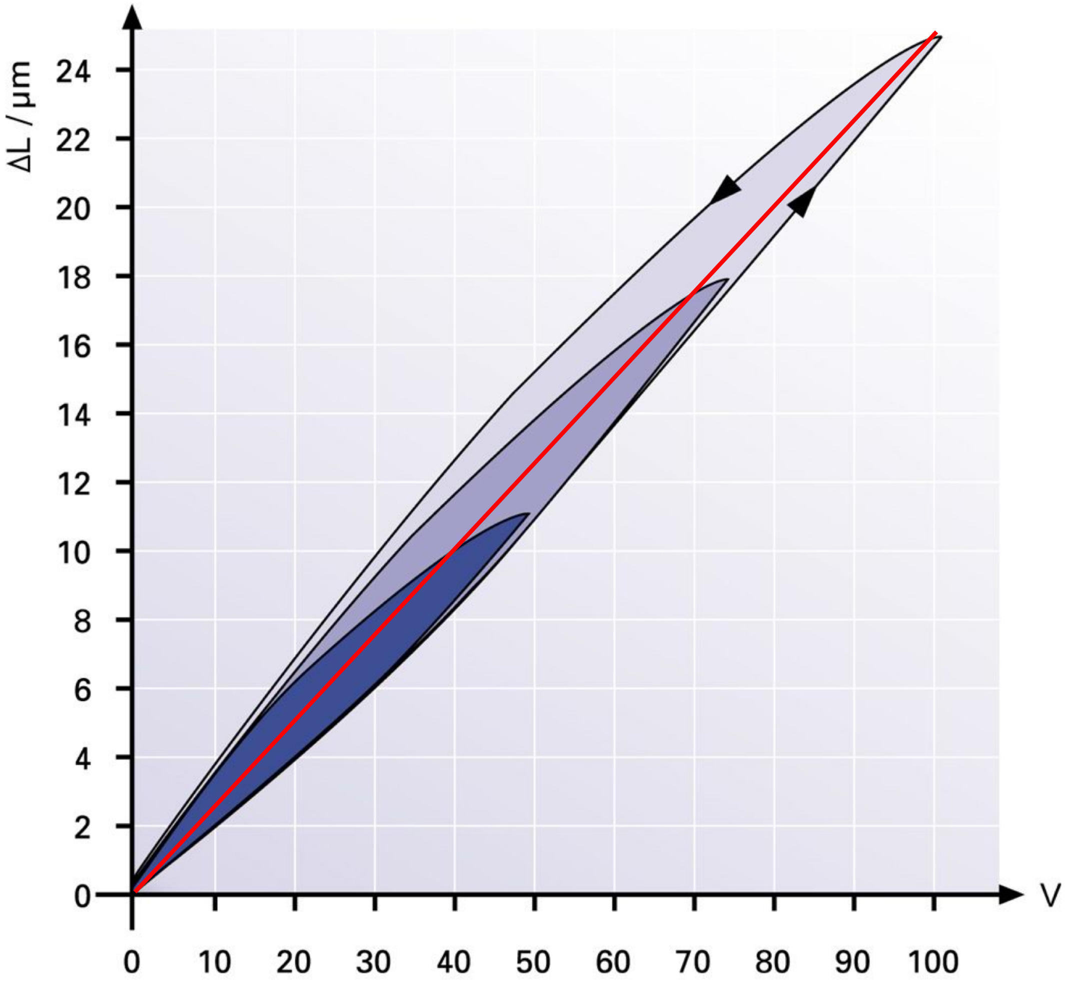

Hysteresis for various peak voltages.

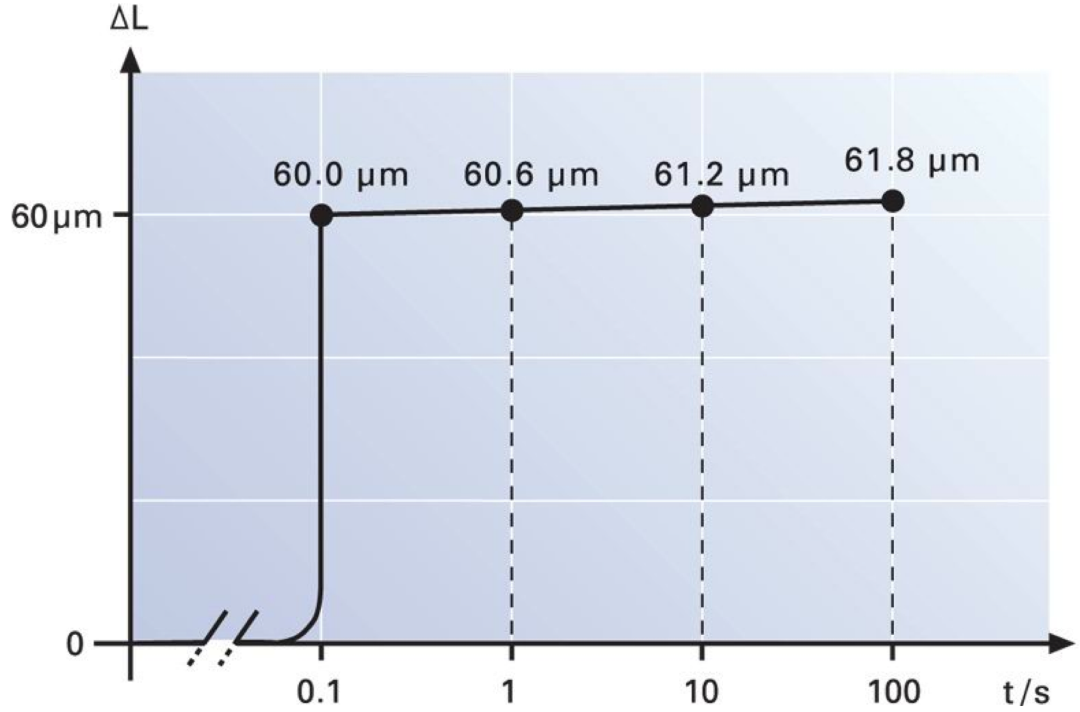

Creep after a (here 60 µm) displacement

$$\Delta L = \Delta L_{t=0.1}\left[1+\gamma \log\left(t/0.1\right)\right]$$

www.physikinstrumente.com/tutorial/index.htmlwww.physikinstrumente.com/tutorial/index.html

Other limitations

High voltage amplifiers noise: about 1 mV over 0 to 5 kHz.
Induced mechanical noise = about 0.1 Å !   (sensitivity 100 Å/V)

Mechanical resonances:

Elongation : $f_{elongation} = \frac{c}{4L}$

Flexion : $f_{flexion} = 0.56 \frac{\sqrt{D^2 + d^2}}{8} \frac{c}{4L^2}$

$c = 3$ km/s, $L = 1$ cm, $d = D = 3$ mm

$f_{elongation} = 10^5$ Hz ; $f_{flexion} = 10^4$ Hz

Aging: re-calibration needed.

Chapter 2
Scanning probes microscopes instrumentation

2.4: Scanning

The scan

Tip is moved to start position, scanned over the surface, and moved back to start position.

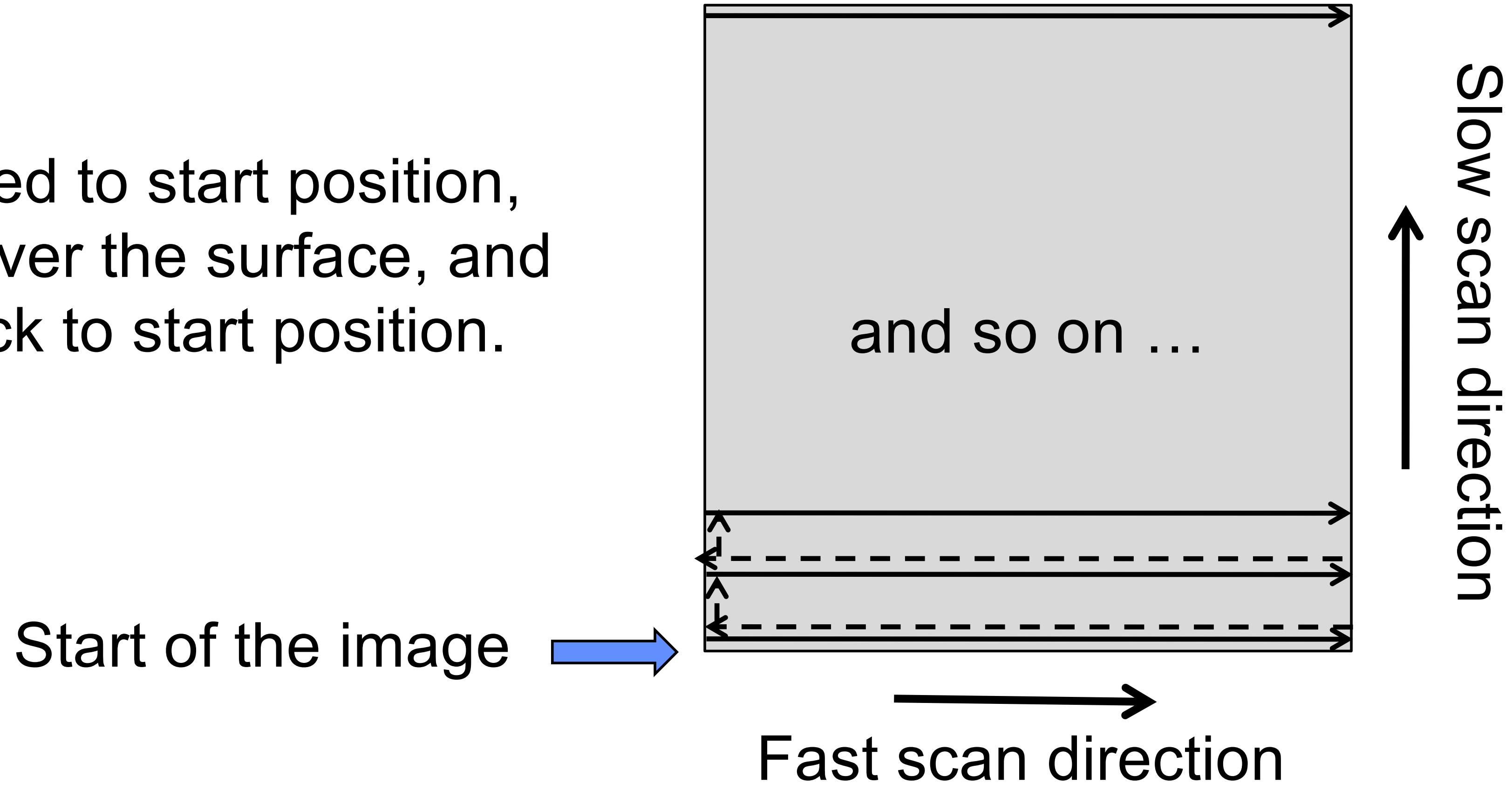

→ Trace: tip is scanned, topography is recorded.

- - - - - → Retrace: tip is scanned back, topography can be recorded also.

Image rendering

Images traced in the hypothesis of a displacement at constant speed

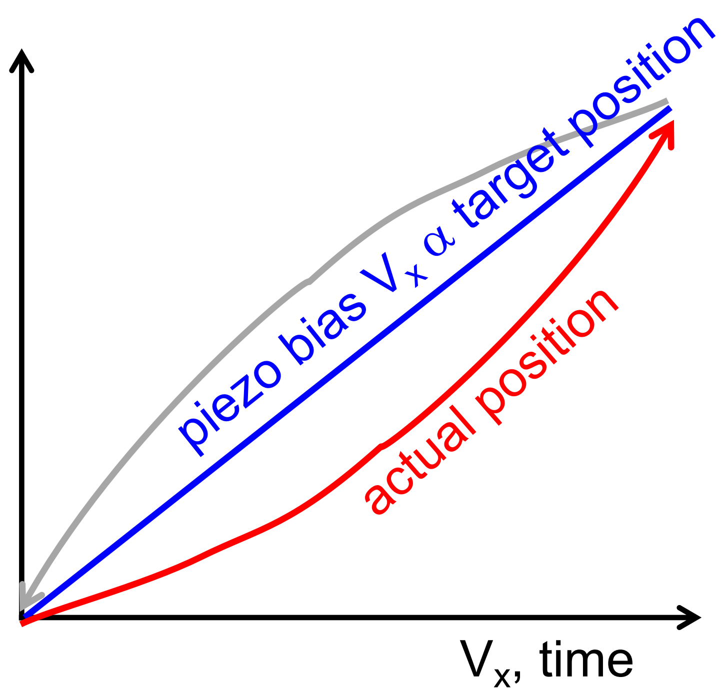

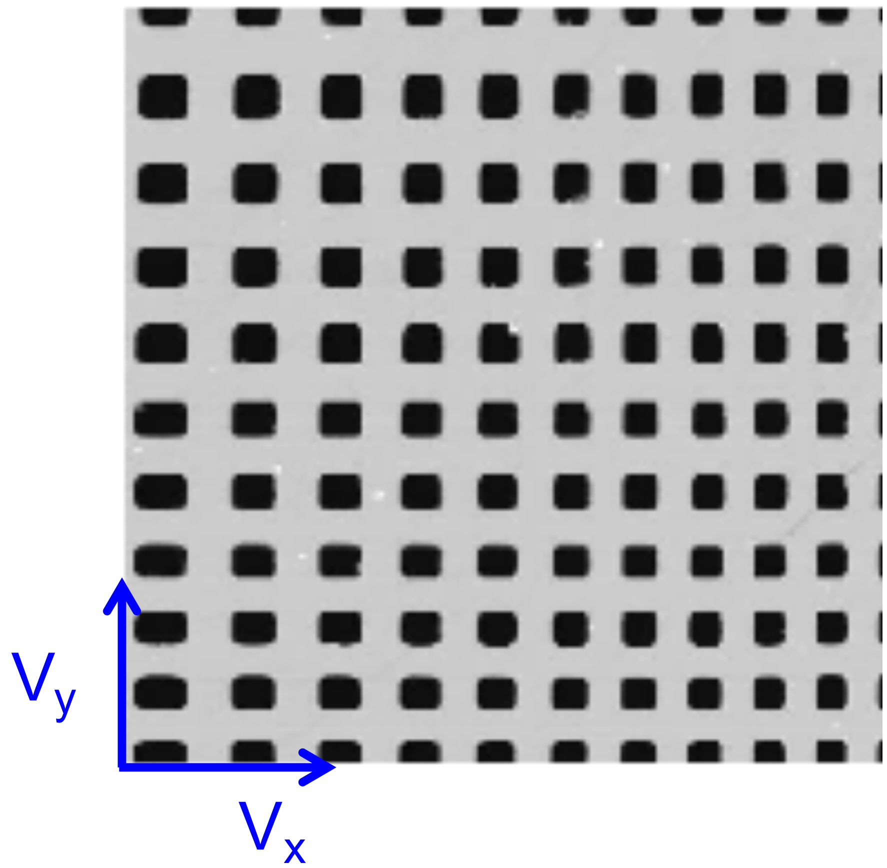

Exemple of hysteresis effect

Images traced in the hypothesis of a displacement at constant speed

Difference between trace and retrace images.

Tip shifted left (right) in the course of the trace (retrace) image.

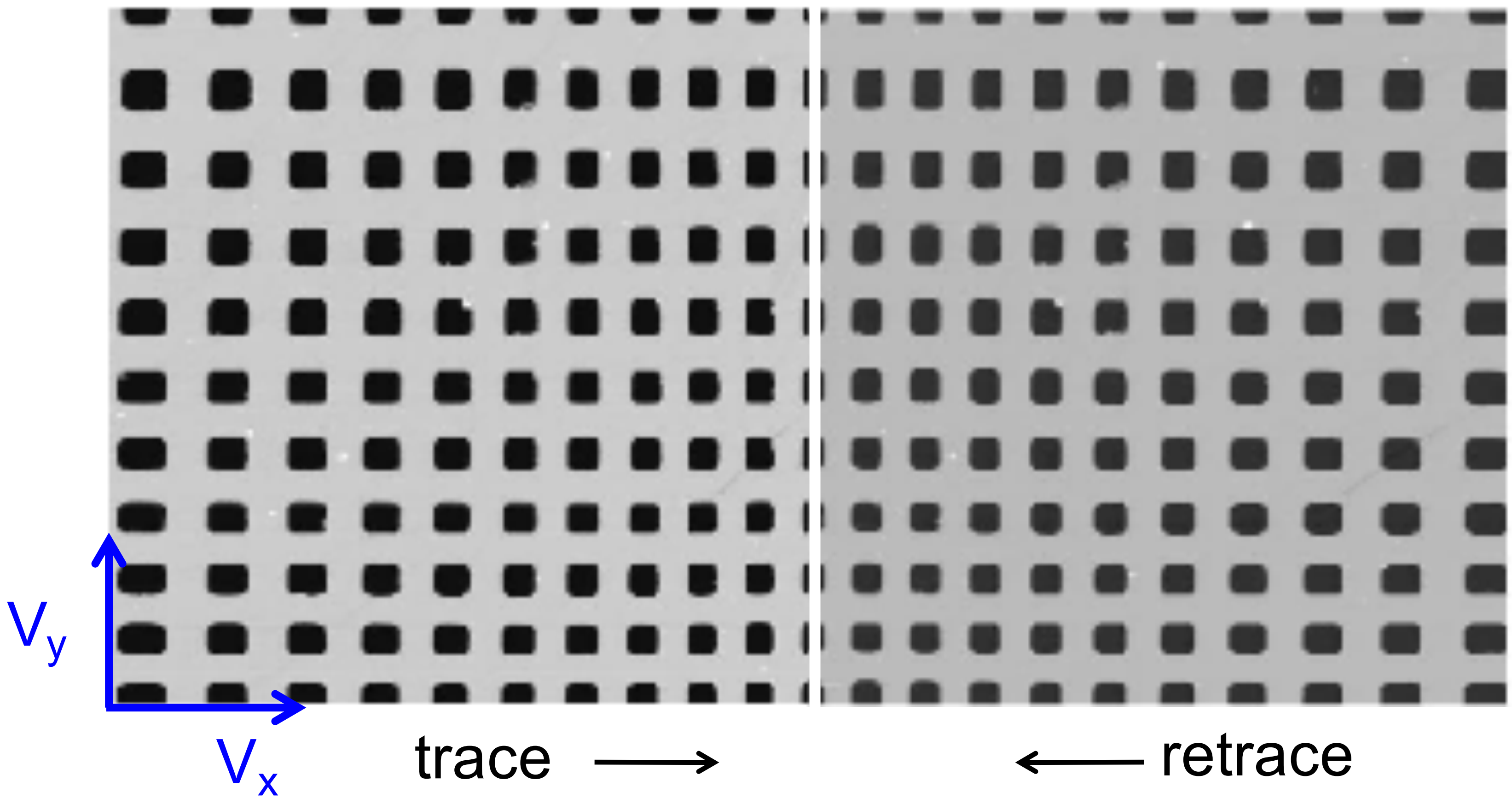

Closed loop operation

Capacitive position sensor

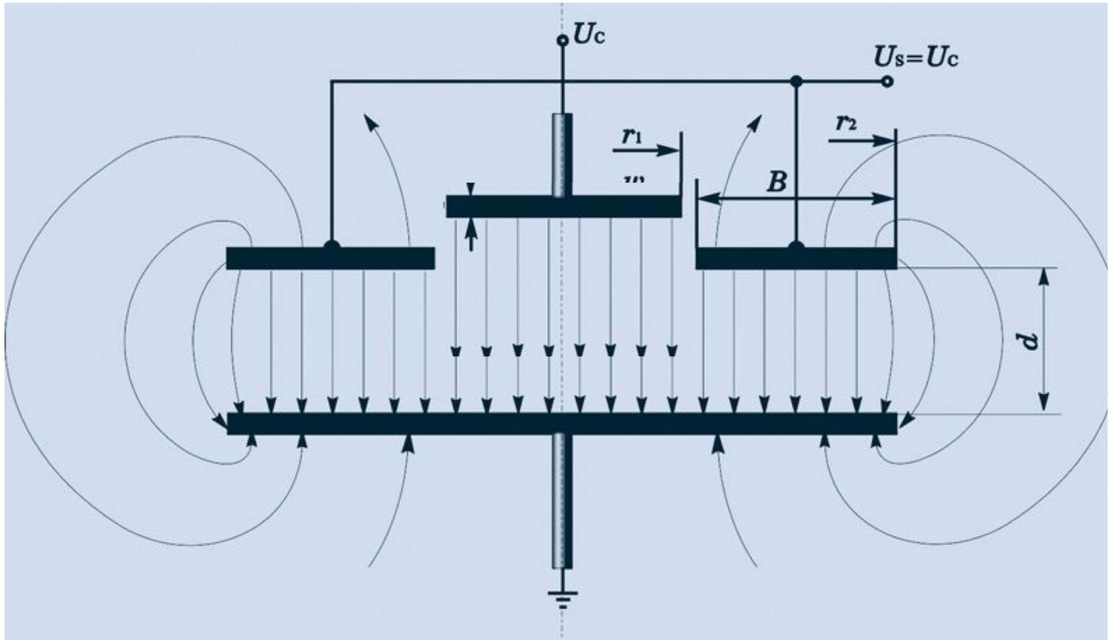

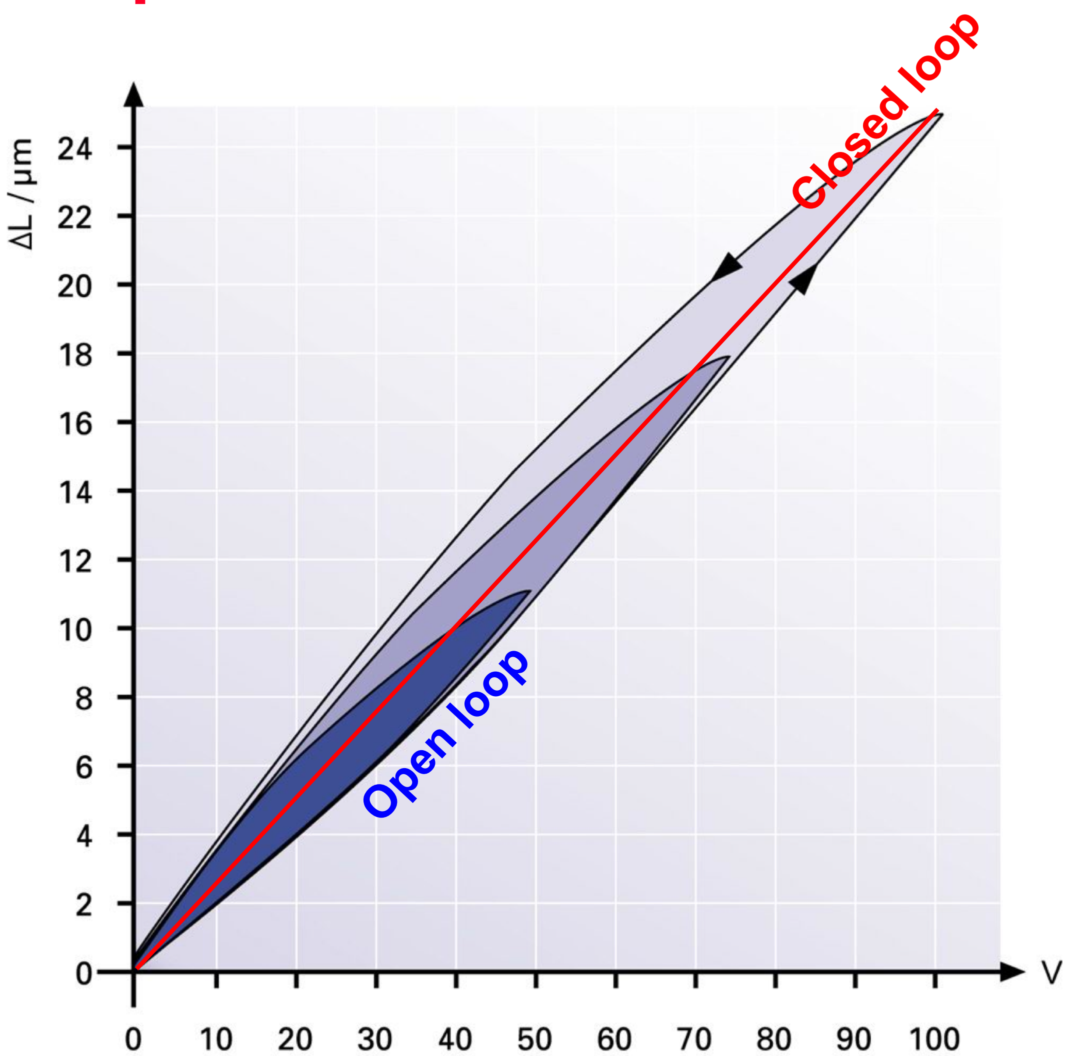

Closed loop operation: actual position is measured and corrected.

Available in various commercial AFMs.

Chapter 2
Scanning probes microscopes instrumentation

2.5: Coarse positioning

how to make approach of a sample towards a tip
(from mmm scale down to nm)

The inertial motor

Wagon on two rods,
non-sliding condition :

$$\frac{T}{N} < f$$

T = ma : tangential part
N : normal part of
the contact force

If $a > \dfrac{fN}{m}$

the wagon slides.
One step = about 10-50 nm.

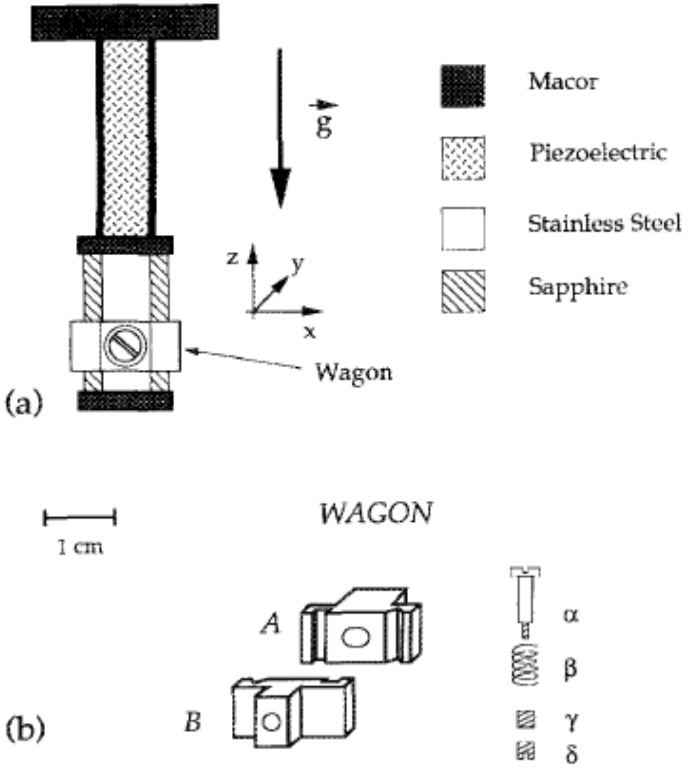

FIG. 1. The vertical translation device with a detailed view of the wagon The screw (α) and spring (β) fit into anvil A, whereas the counterpiece (γ) and the blocking screw (δ) are screwed into anvil B.

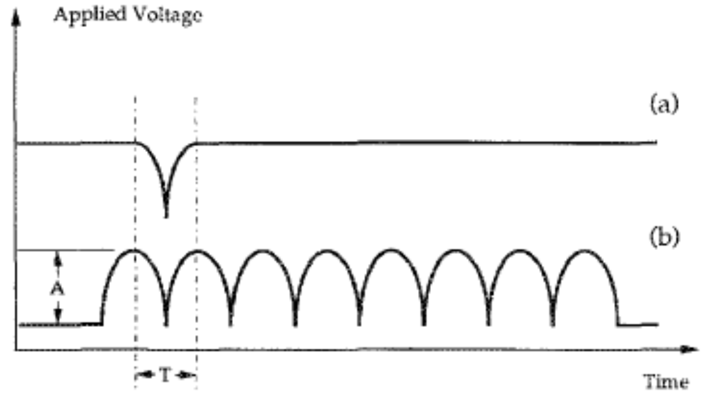

FIG. 2. Cycloidal functions required to move the wagon upwards: (a) single step; (b) continuous stepping.

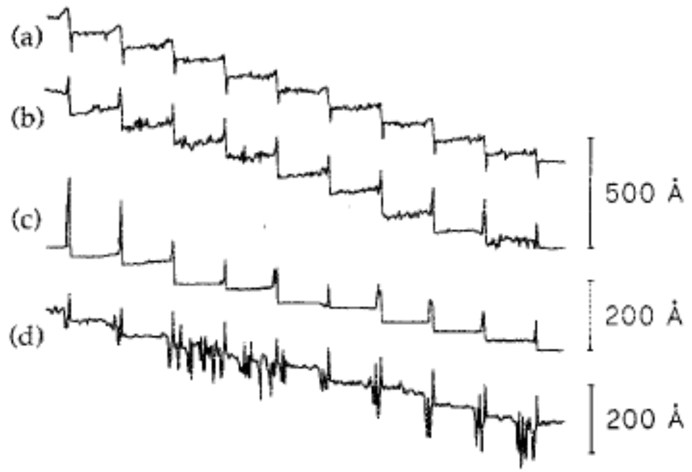

FIG. 3. Tunneling probe recording of single steps against gravity: (a) in air at room temperature, $A = 33.5$ V, $f = 800$ Hz; (b) in He gas at 77 K, $A = 37.1$ V, $f = 800$ Hz; (c) in air at room temperature, $A = 15$ V, $f = 5.5$ kHz; (d) in He gas at 77 K, $A = 35.6$ V, $f = 800$ Hz ($f = 1/T$).

C. Renner et al., Rev. Sci. Instrum. 61, 965 (1990).

Example of commercial inertial motors

From Attocube company:

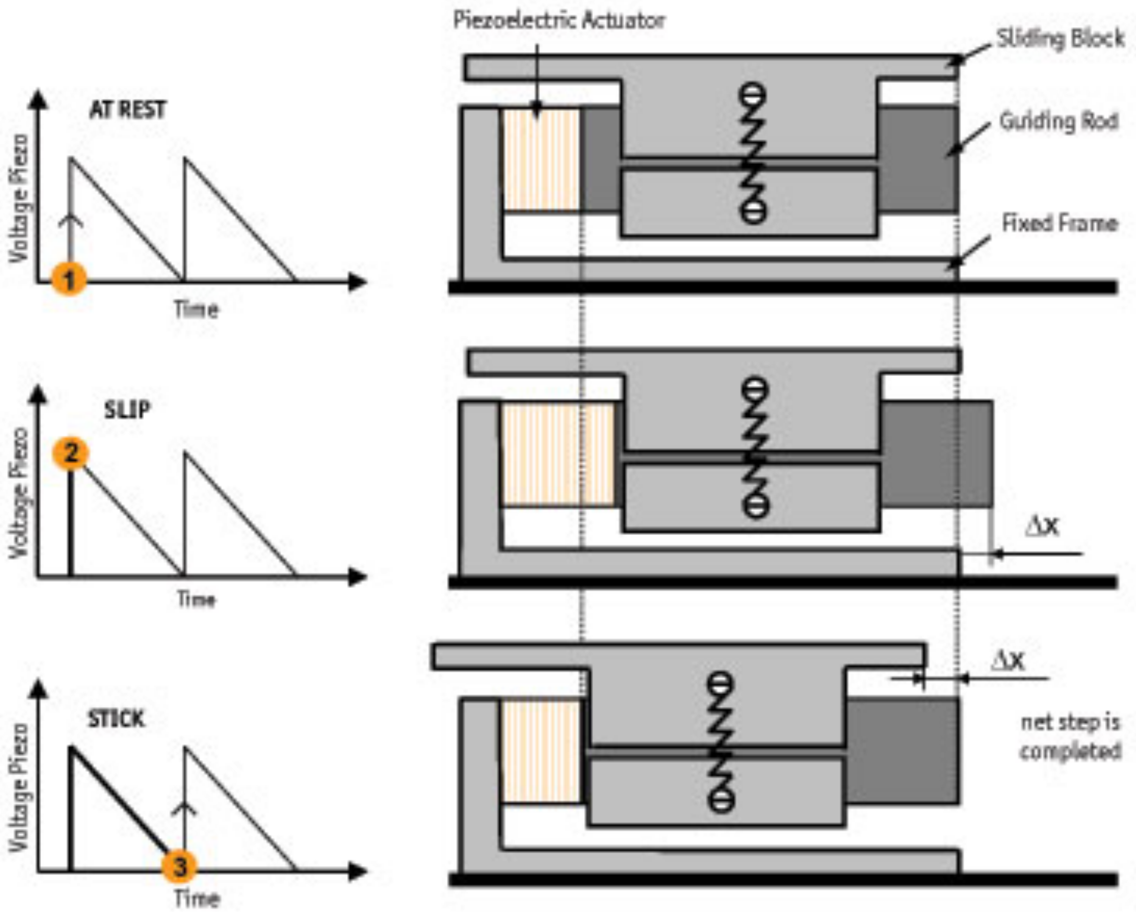

The Pan motor

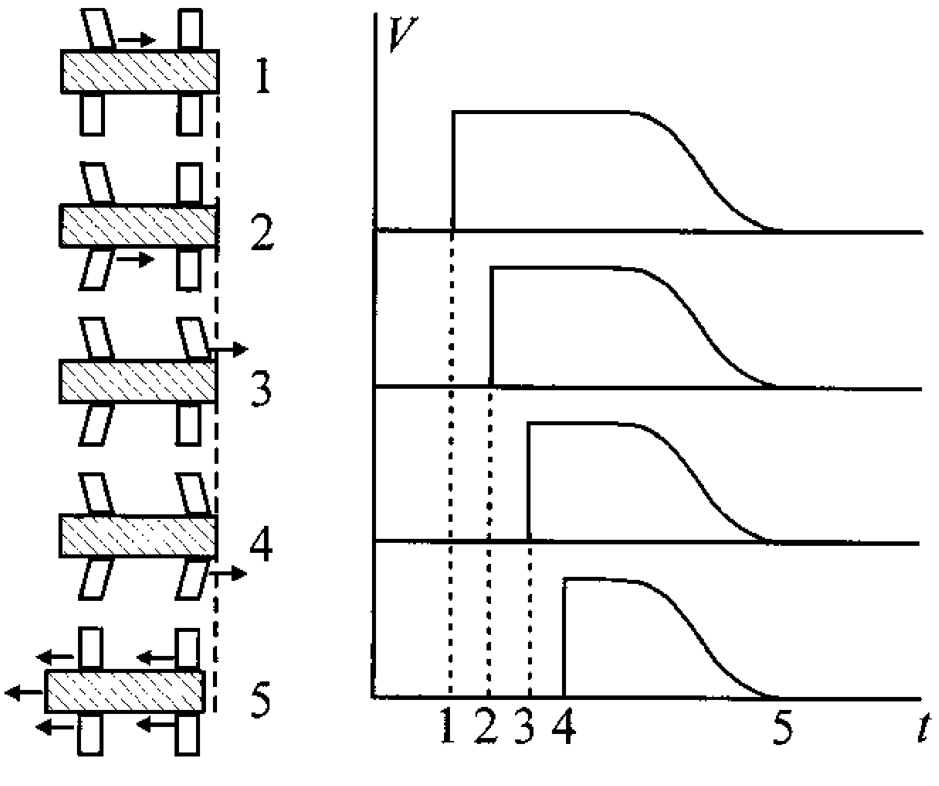

(a) (b)

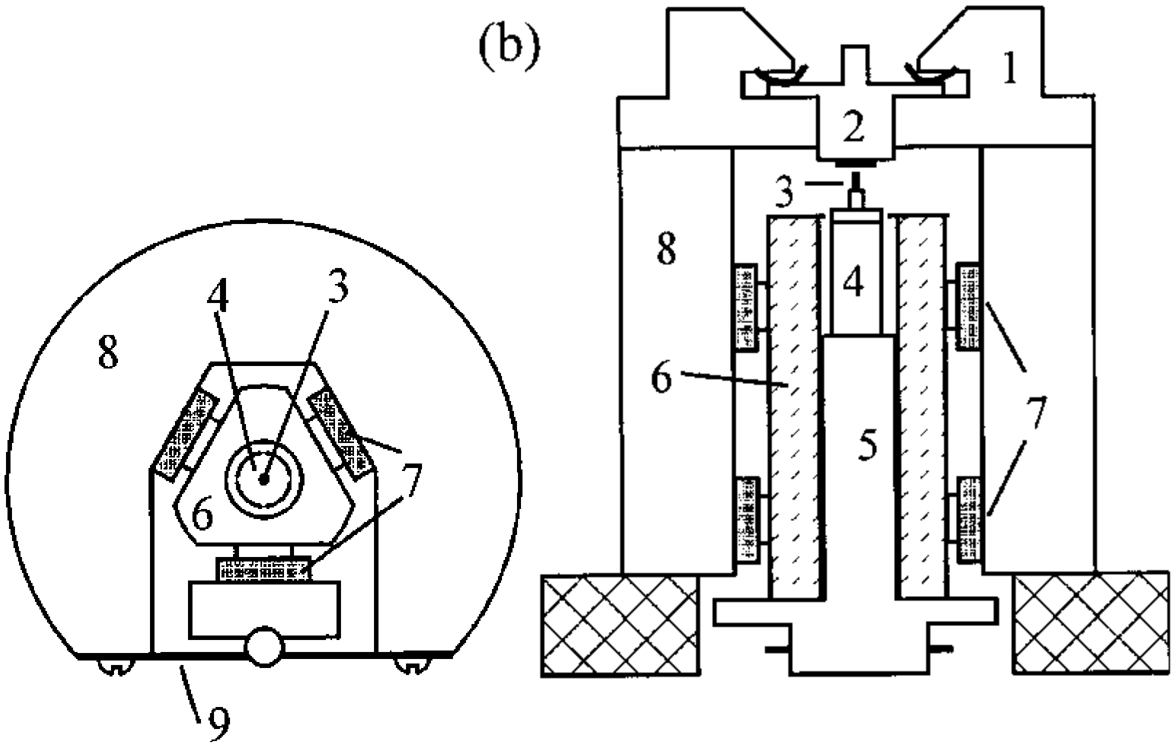

top view with sample receptacle removed for clarity and side view. 1.5 in. in diameter by 1.75 in. high. (1) Sample receptacle, (2) sample holder, (3) tip, (4) tube scanner, (5) scanner holder, (6) sapphire prism, (7) shear piezo stacks, (8) macor body, (9) spring plate (not to scale).

Based on shear piezos. Walker (inchworm) regime: leg by leg movement, 3 stick more than 1. Retraction of the 4 legs together.

Can also be operated in the inertial regime (4 legs pulsed together).

S. Pan et al, Rev. Sci. Instrum. 70, 1459 (1999).

Stepper motors

Present in most commercial AFMs, accuracy down to 30 nm.

The electromagnet 1 is turned on, aligning the nearest rotor teeths with the stator teeths. At this point, the rotor are slightly offset from electromagnet 2 teeths. The electromagnet 2 is turned on, …

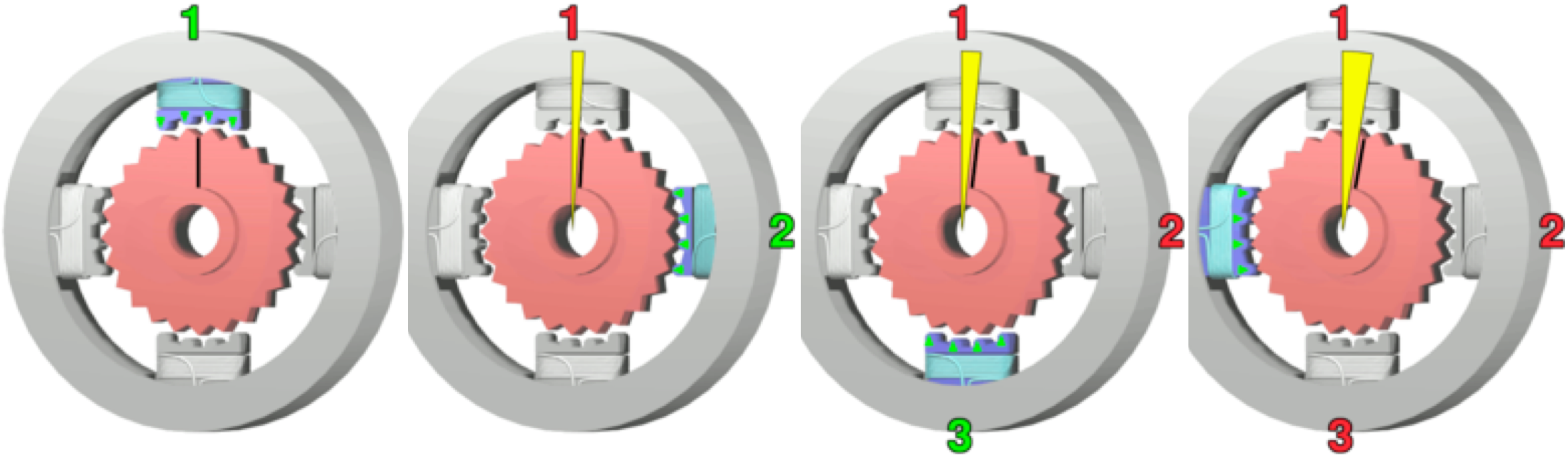

Here 25 teeths on rotor, on stator period corresponding to 24 teeths, rotation of 360° /(25x4)=3.6° per cycle.

Works usually only in ambiant conditions (grease needed).

Chapter 2
Scanning probes microscopes instrumentation

2.6: Design rules and examples

Vibration isolation

O. Züger, H. P. Ott, and U. Dürig, Rev. Sci. Instrum. 63, 5634 (1992).

x_M = difference between tip and base positions: $x_M(t) = x_{M0}\sin(\omega t + \varphi')$

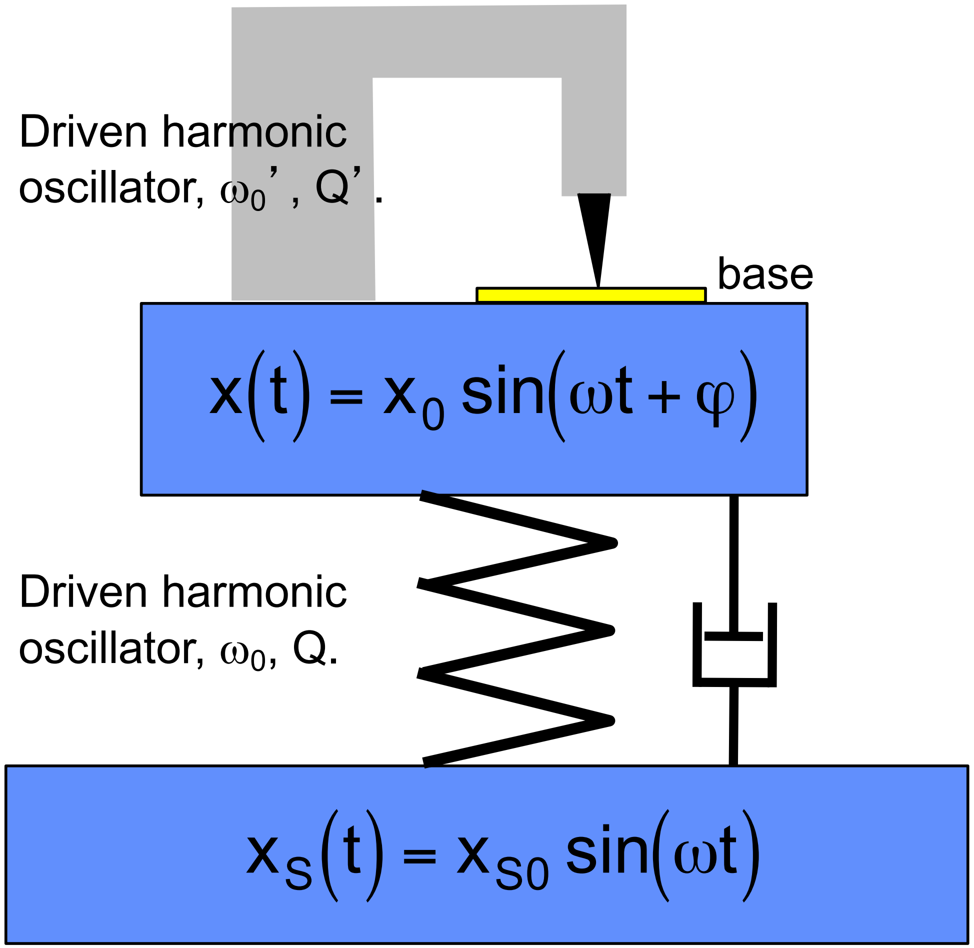

high-pass

$$T_S = \left|\frac{x_{M0}}{x_0}\right| = \frac{\left(\frac{\omega}{\omega_0'}\right)^2}{\sqrt{\left(1-\left(\frac{\omega}{\omega_0'}\right)^2\right)^2 + \left(\frac{\omega}{Q'\omega_0'}\right)^2}}$$

low-pass

$$T = \left|\frac{x_0}{x_{S0}}\right| = \sqrt{\frac{1+\left(\frac{\omega}{Q\omega_0}\right)^2}{\left(1-\left(\frac{\omega}{\omega_0}\right)^2\right)^2 + \left(\frac{\omega}{Q\omega_0}\right)^2}}$$

Incoming vibrations / mechanical damping. Practical limitation: $f_0 > 2$ Hz

Need for a double stage isolation

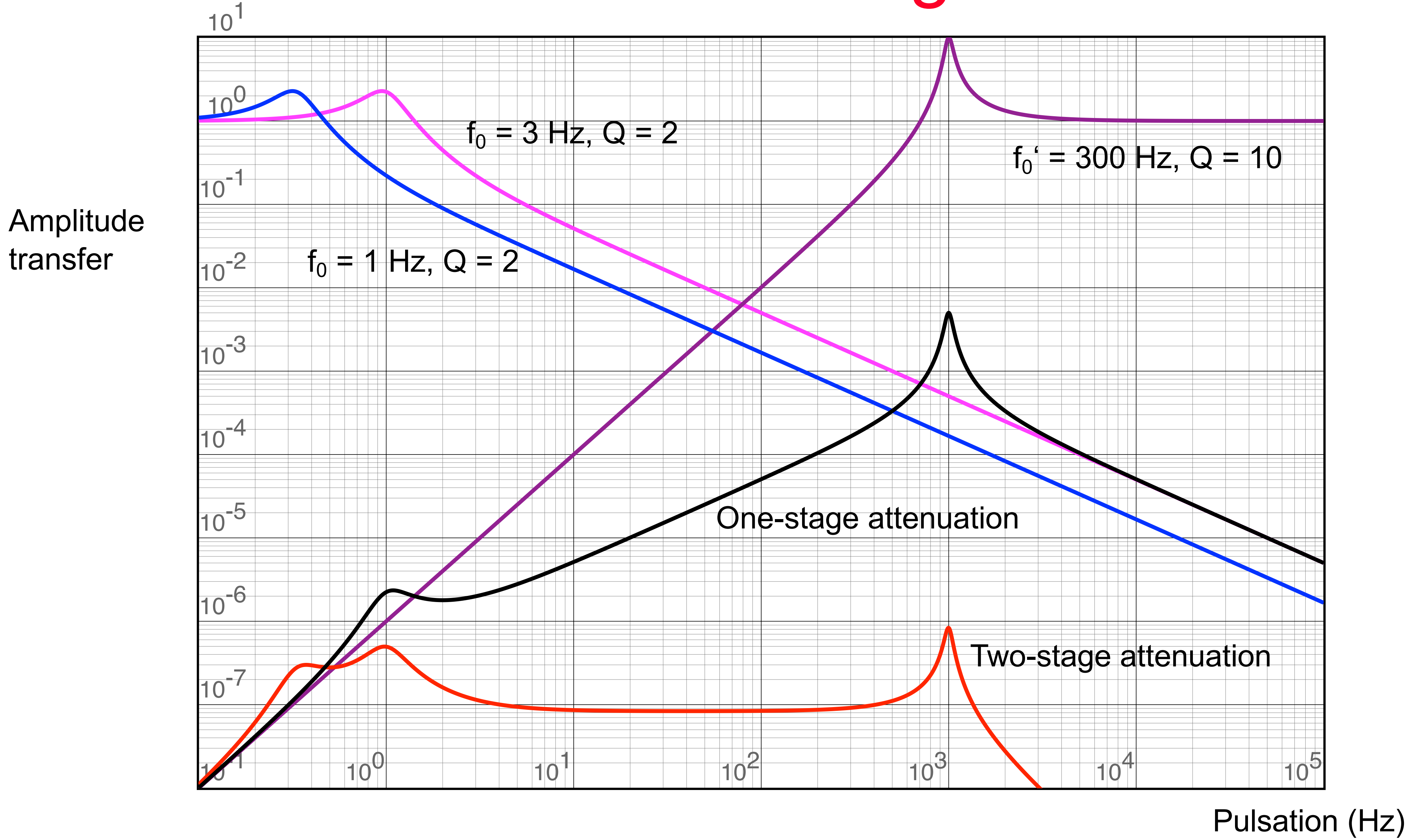

With a 1 µm vibration source at 1 kHz, a 10^{-6} transfer amplitude gives here a 1 pm vibration on the microscope. 10^{-3} gives 1 nm = 10 Å.

Very low-temperature AFM-STM with positioning motors

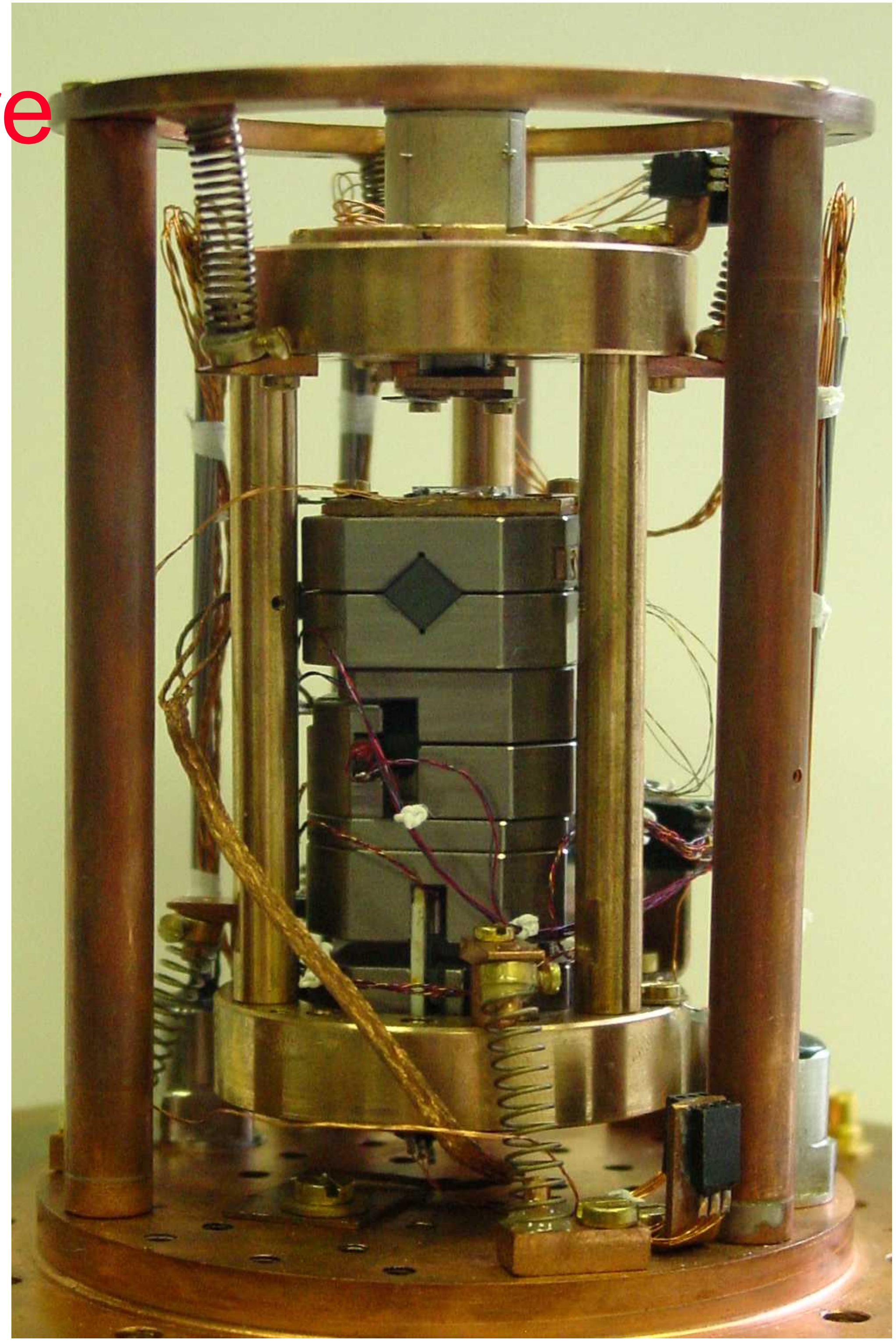

Very low temperature (60 mK) AFM-STM with Attocube motors

Th. Quaglio, F. Dahlem, S. Martin, A. Gérardin, C. B. Winkelmann and H. Courtois, Rev. Sci. Instrum. 83, 123702 (2012).

The beetle geometry

Coarse approach based on the displacement of the 3 feet along a ramp.

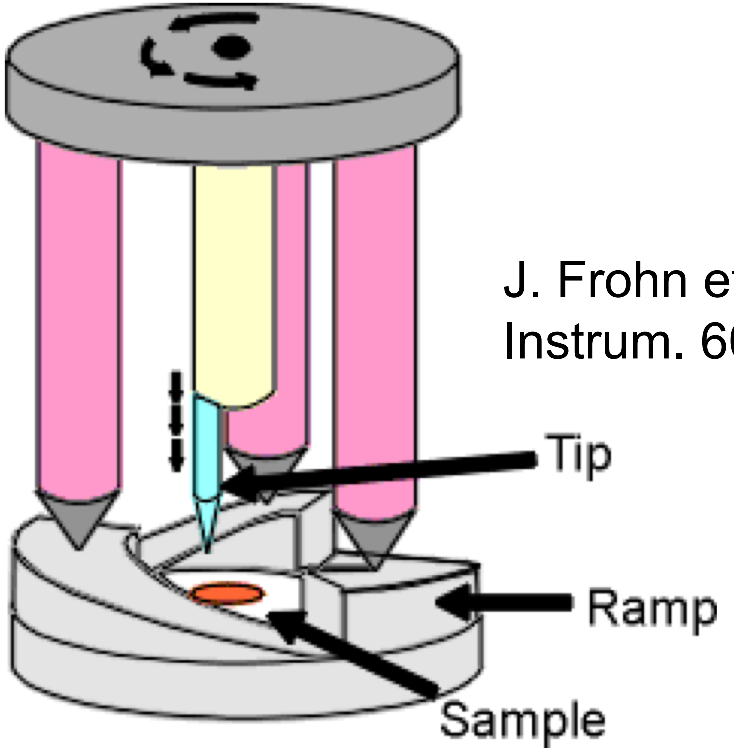

J. Frohn et al., Rev. Sci. Instrum. 60, 1200 (1989).

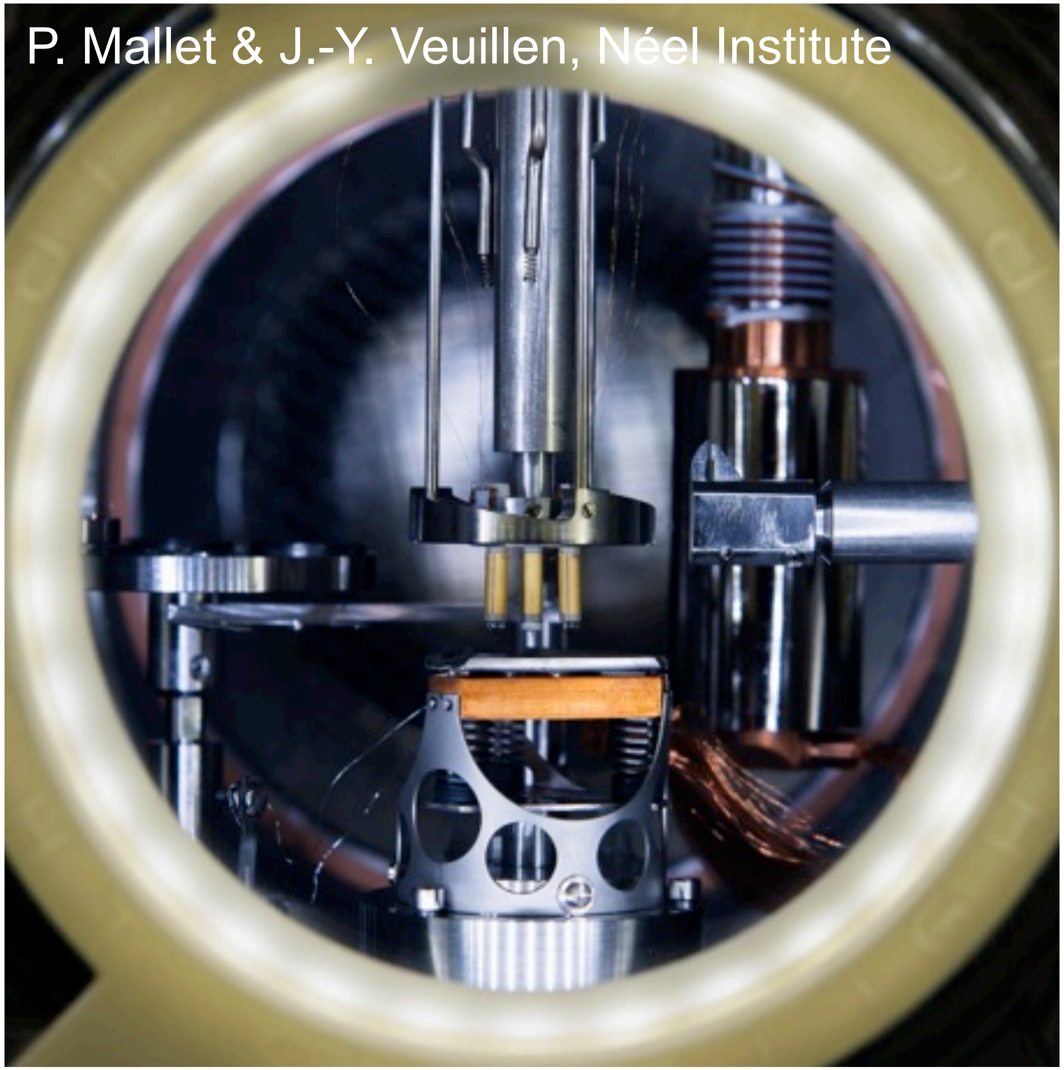

Well adapted to ultra-high vacuum (UHV) systems.

Excellent access to sample and tip.

Veeco microscope (at CIME)

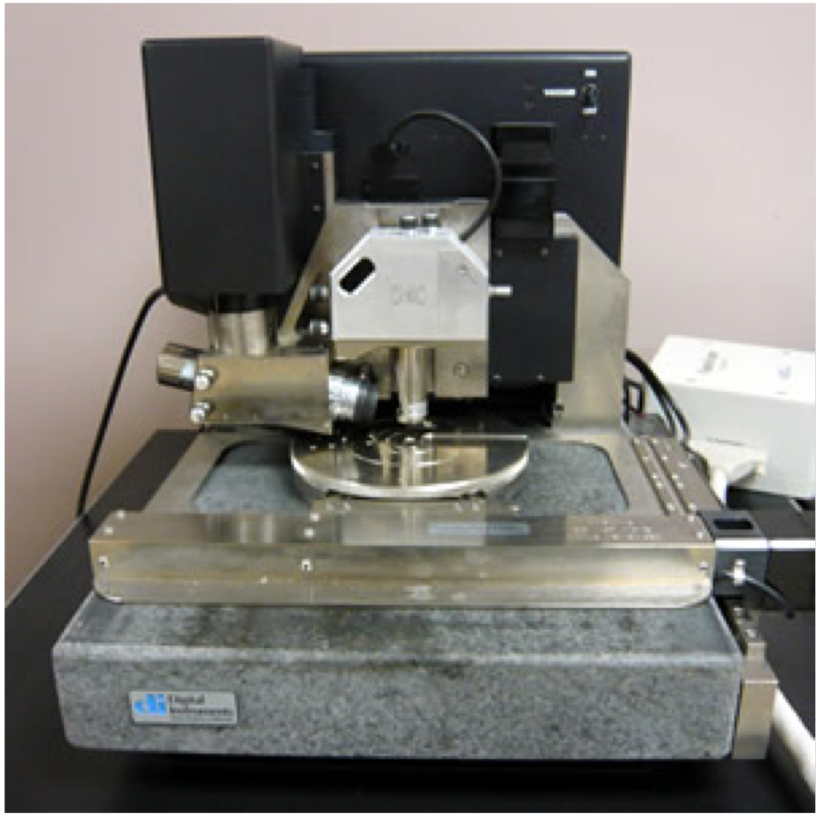

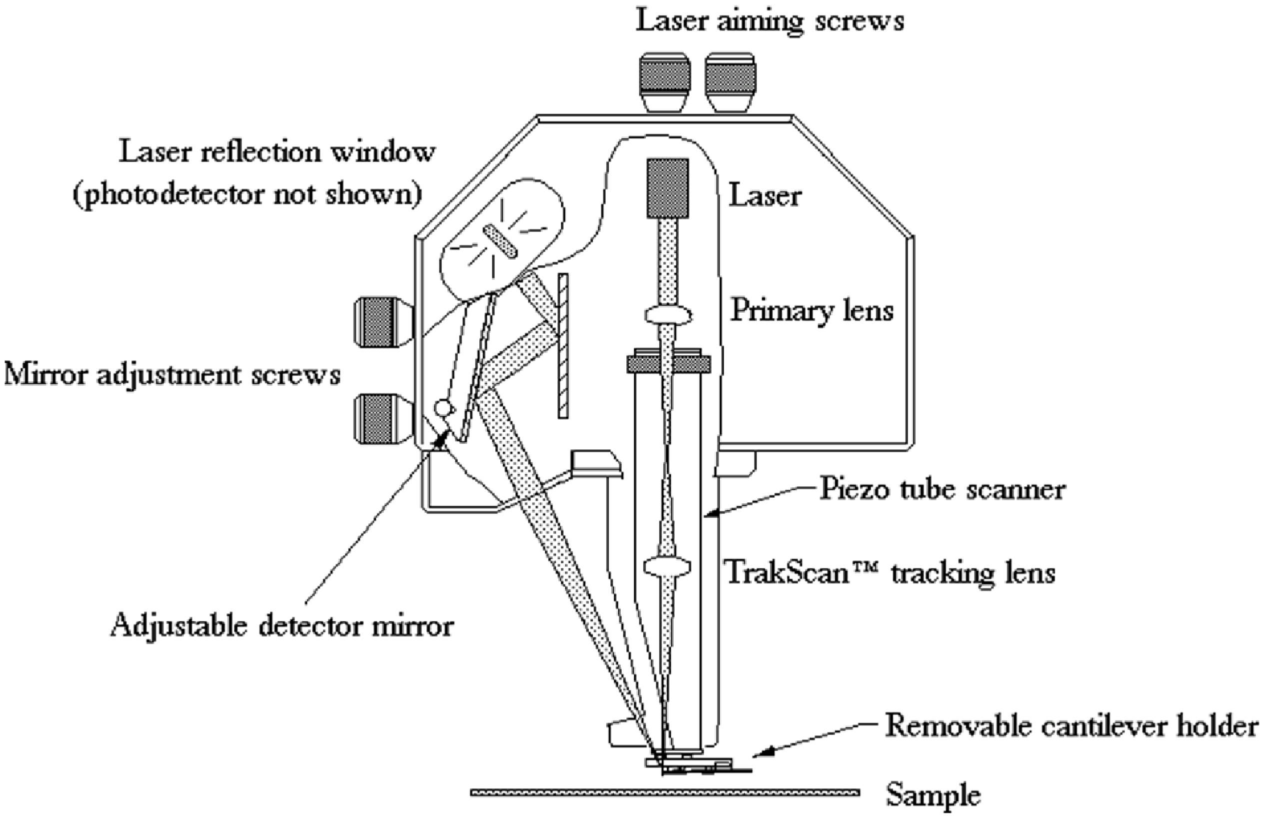

Piezo tube for tip scanning
Stepper motors for sample coarse positioning.

Chapter 2
Scanning probes microscopes instrumentation

2.7: SPM control

STM control electronics

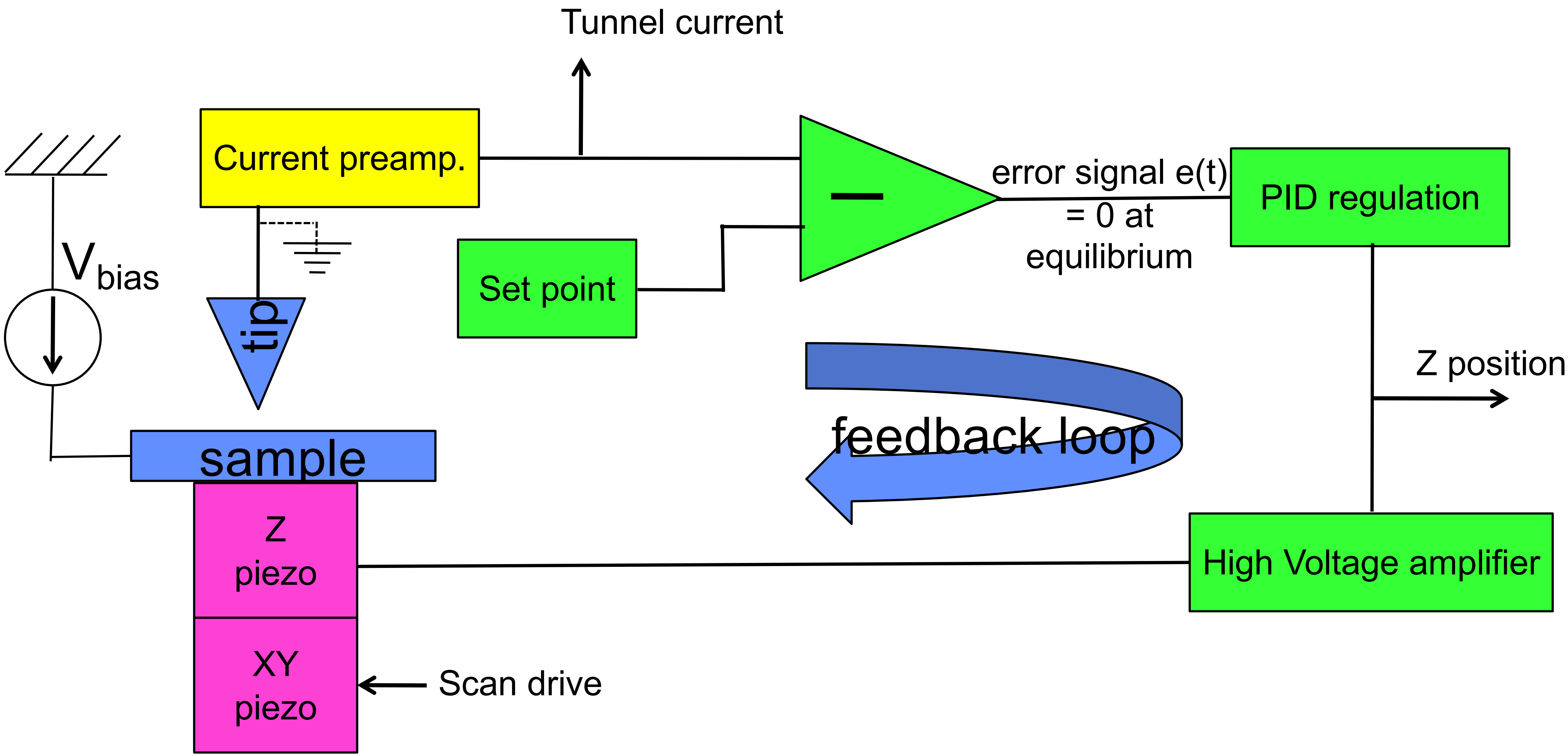

Here, the sample is scanned. It could be the tip, no difference.

The tunnel current measurement

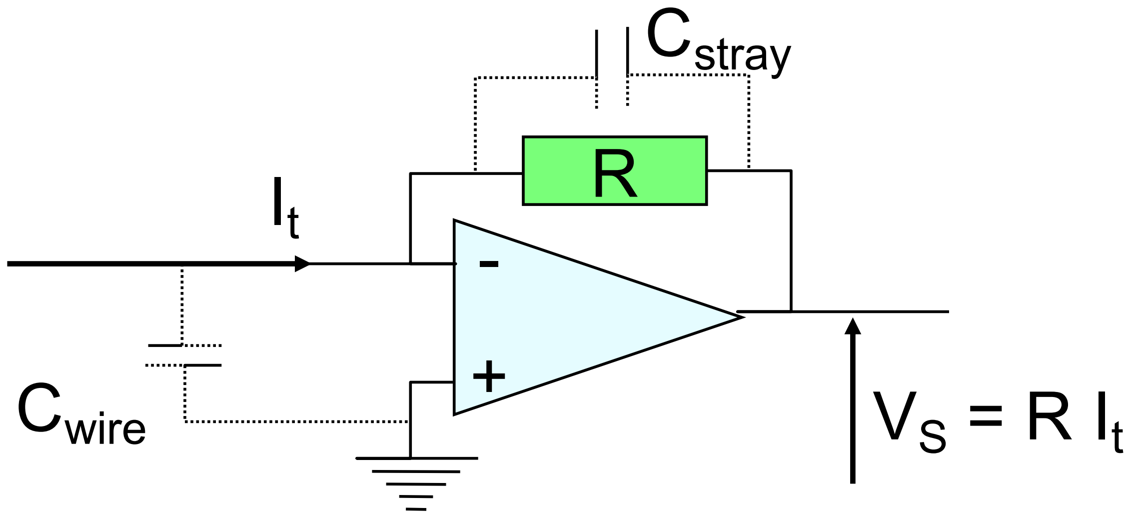

R = 100 MΩ usually
1 nA -> 0.1 V

Bandwidth = $1/RC_{stray} = 10^8.10^{-12} = 10^{-4}$ s
Op-amp noise = current noise + voltage noise/wire-ground impedance

$$i_{OA} = i_{noise} + C_{wire}\omega v_{noise}$$

about 5 nV/Hz$^{1/2}$

Thermal noise of the resistance R :

$$P_{noise} = 4k_B T\Delta f \Rightarrow i_{Johnson} = \frac{\sqrt{4k_B T\Delta f}}{R} \approx 0.3\text{pA} \quad \text{in } [0;3\text{kHz}]$$

The PID regulation

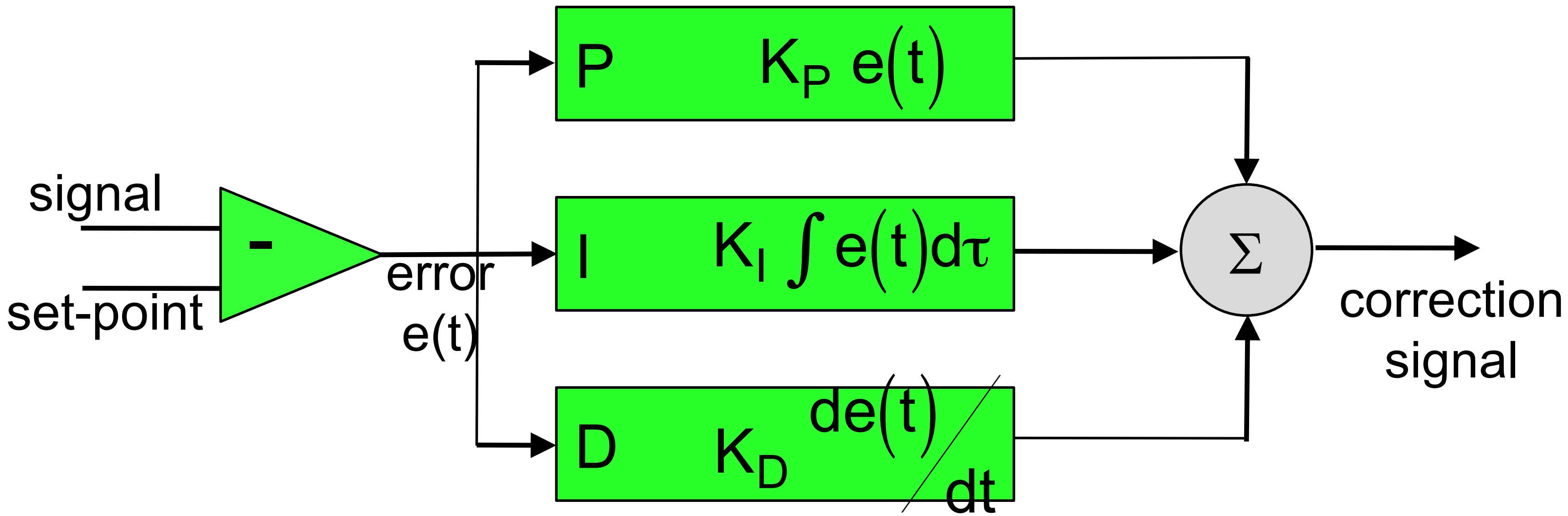

P, I and D signals generated analogically with op-amps or digitally.

The PID regulation (2)

Strong K_P for large gain, strong K_I to accelerate the response

Ziegel-Nichols coefficients setup procedure: increase K_P until oscillations appear, reduce K_P to 0.45 of this critical value, set K_I to 0.85 the oscillation period. K_D little useful. J. Ziegel, N. Nichols, Trans. ASME 64, 759 (1942).

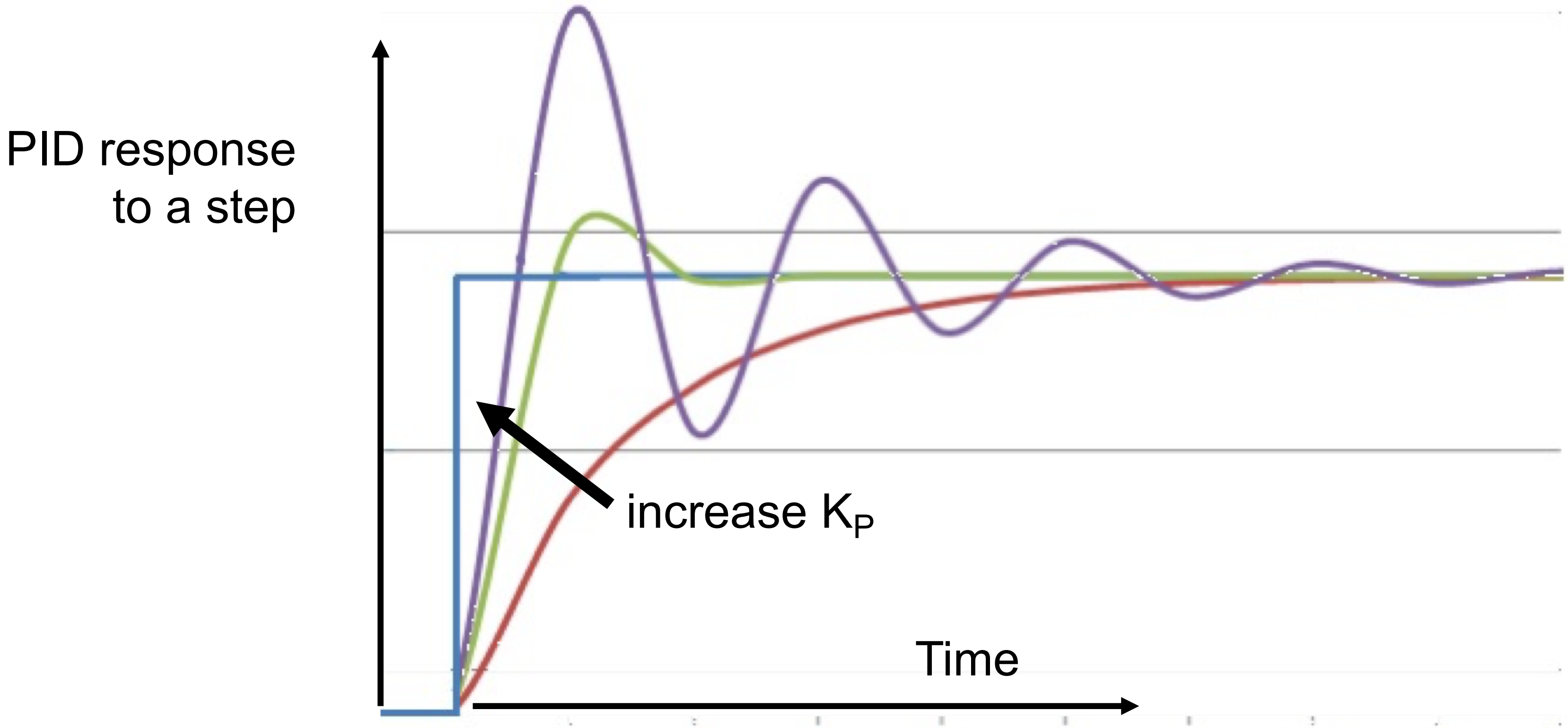

Feedback and error signal

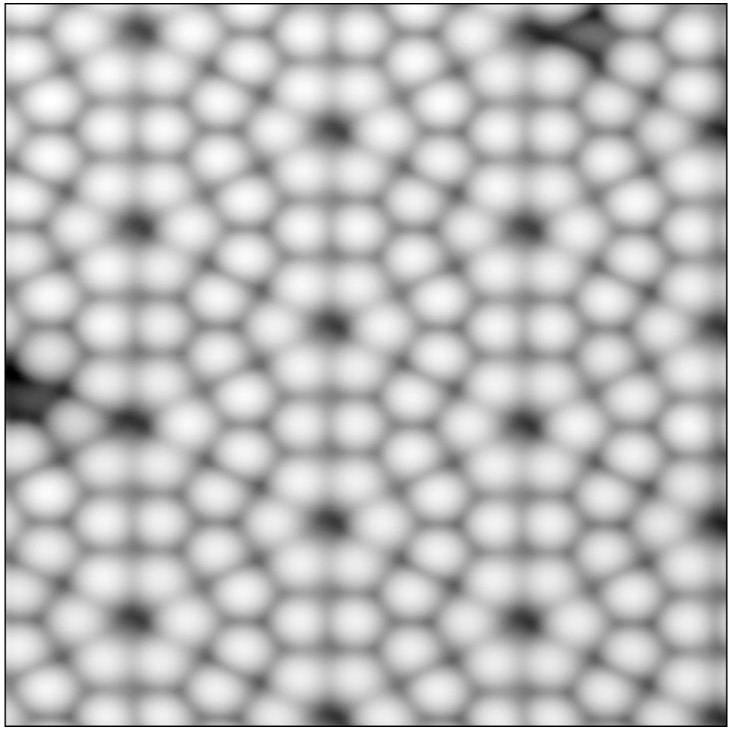

topography $\Delta z = 0.2$nm
„image“

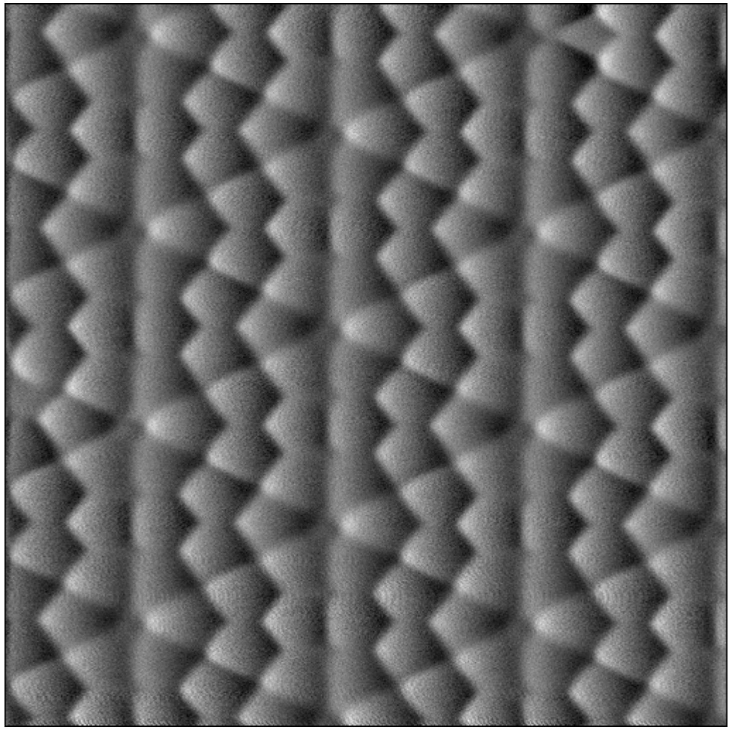

$I_T = 0.5$nA; $\Delta I_T = 0.18$nA;
„error signal“

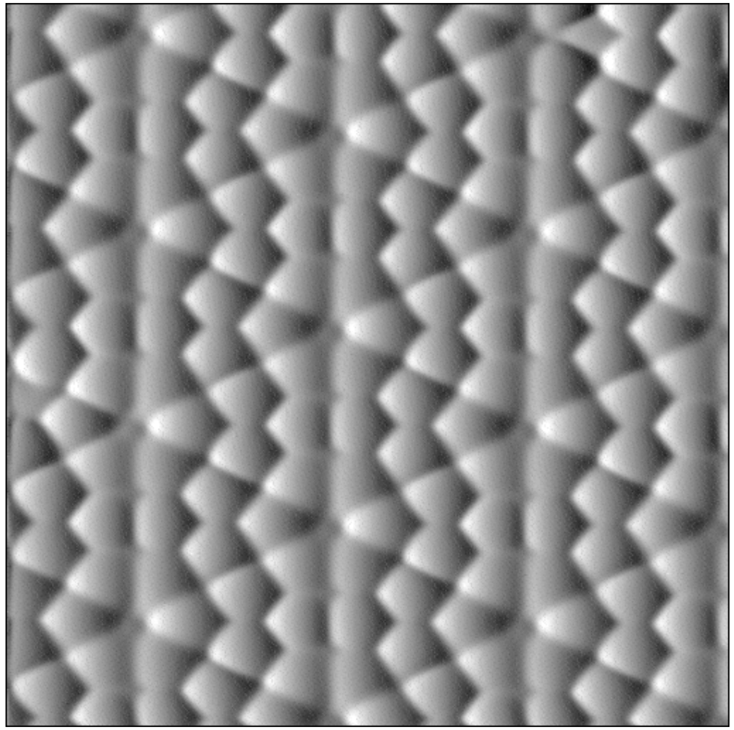

dz/dx derivative
„simulated error signal“

A feedback is like a low-pass filter
High frequencies appear in the error signal, that looks like the derivative of the feedback.
Faster scanning or slower feedback generates larger errors

SPM control electronics

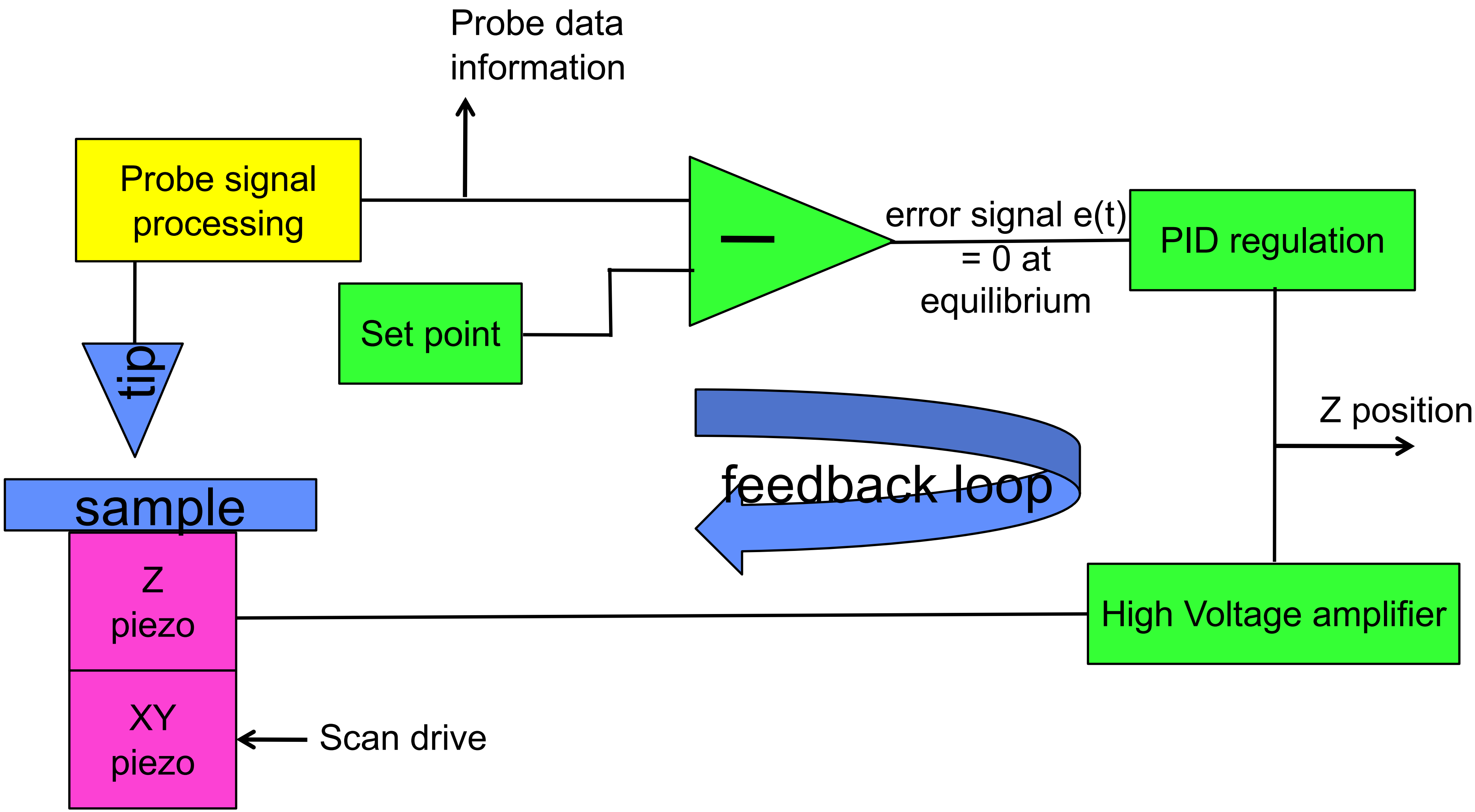

Electronics can be analog or digital.